Wavefront Estimation and Control: Ground

Donald Gavel
UCO/Lick Observatory
Laboratory for Adaptive Optics

Michelson Summer School – High Contrast Imaging in Astrophysics

July 21, 2004

Outline

- Purpose and requirements of ground-based adaptive optics
- Technologies for atmospheric AO
- Measuring wavefronts
- Controlling wavefronts
- High contrast imaging challenges

Adaptive optics

1. Correct for atmospheric turbulence
2. Secondary outcome: correct for imperfect telescope optics

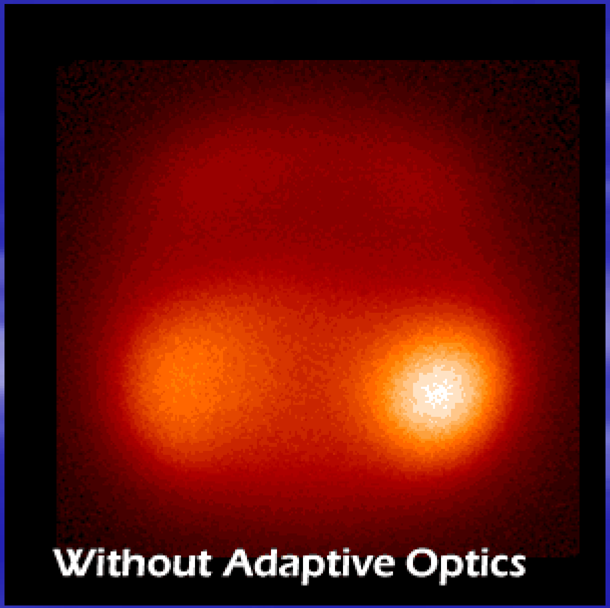

Diffraction-limited image formation

$$\sigma_\varphi = \left\langle \left[\phi(\mathbf{x}) - \frac{1}{A} \int_{pupil} \phi(\mathbf{x}) dx \right]^2 \right\rangle^{1/2} < \frac{\pi}{2}$$

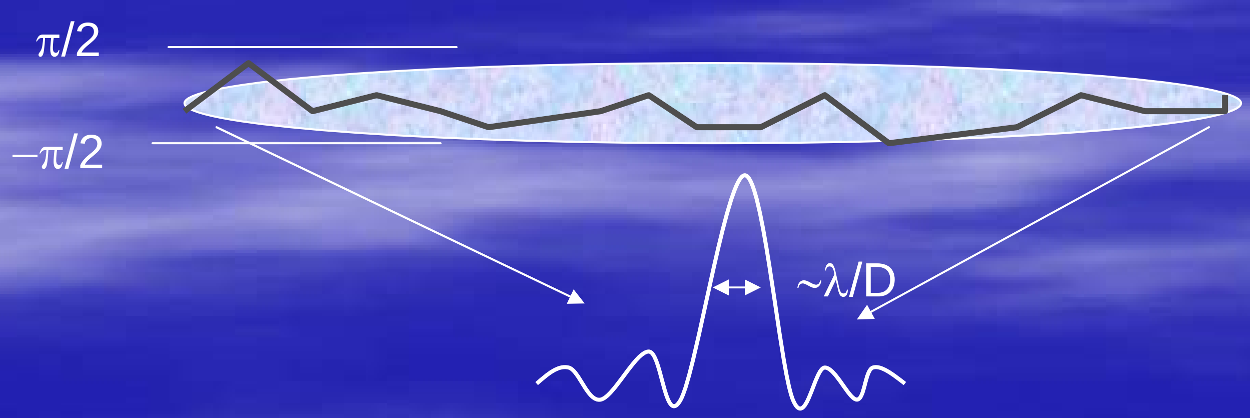

Atmospheric aberrations

Images of a bright star, Arcturus

Lick Observatory, 1 m telescope

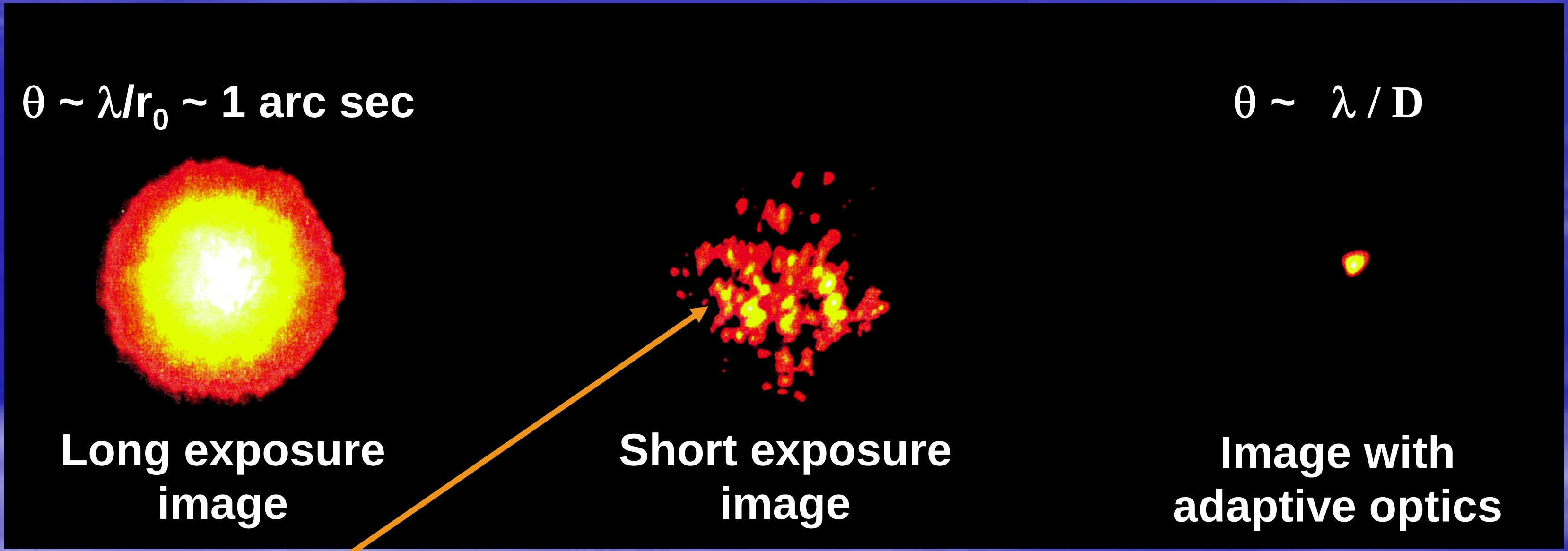

Speckles (each at diffraction limit of telescope)

Aberations arise from turbulent mixing in atmospheric layers

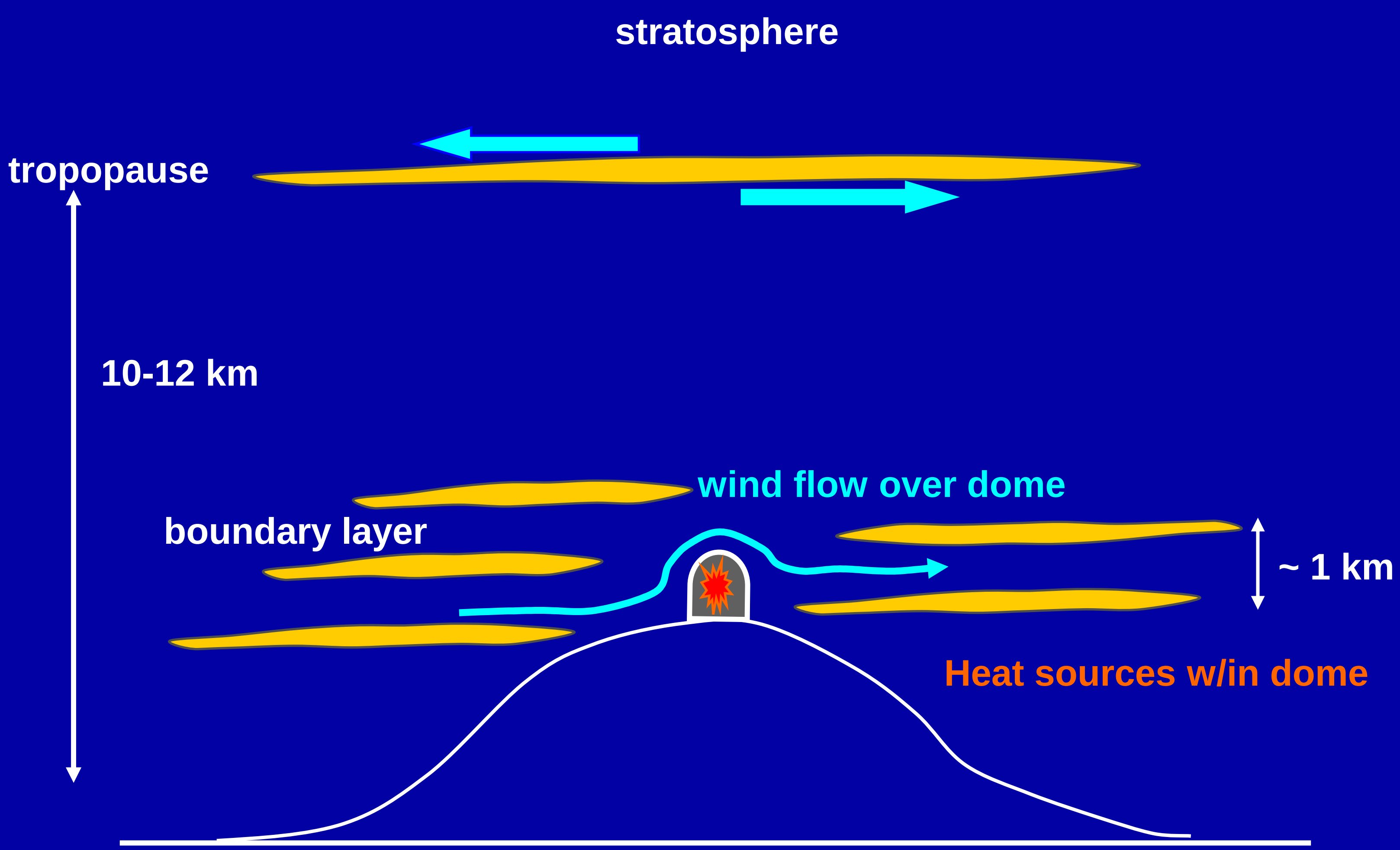

"Typical" $C_n{}^2$ profile of atmospheric turbulence

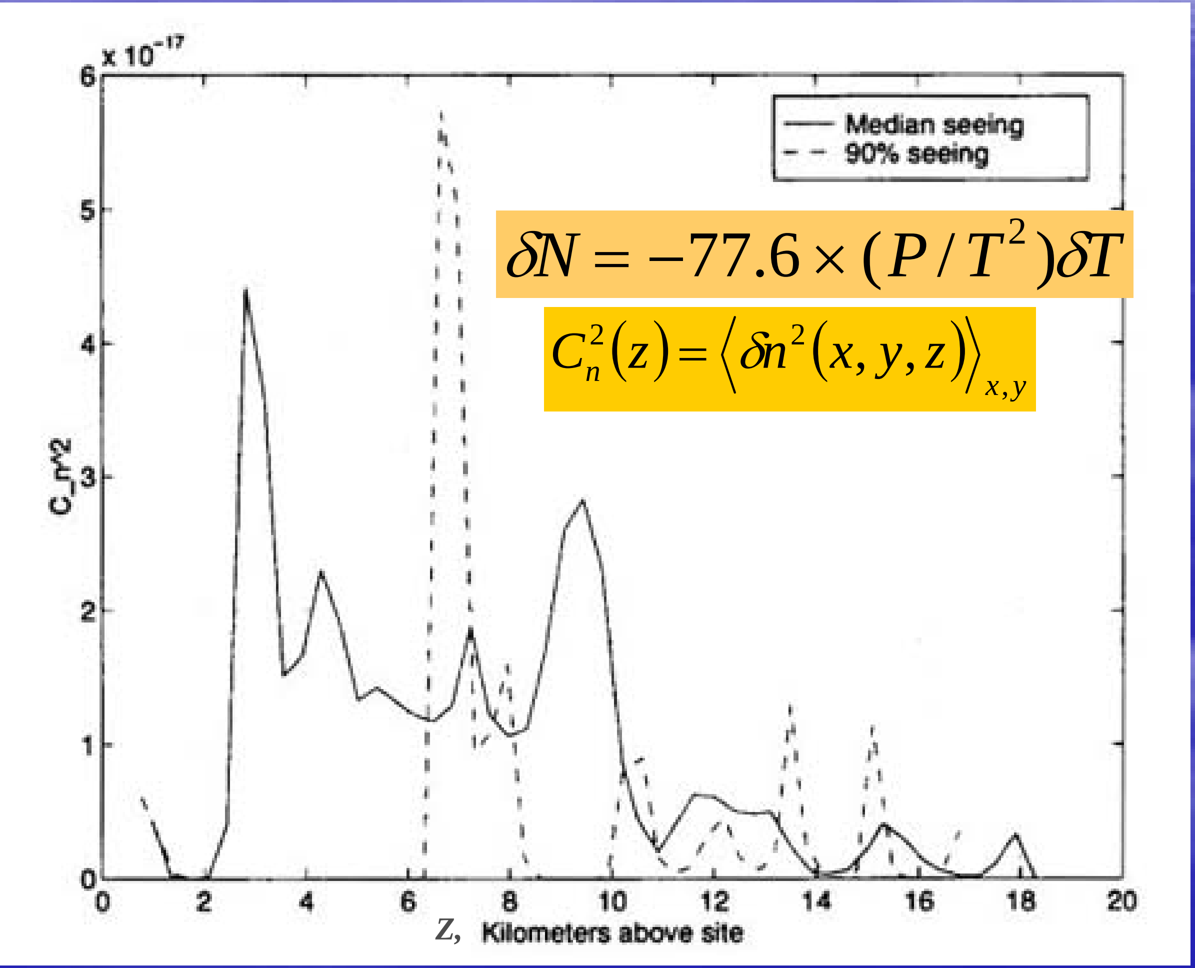

$$\delta N = -77.6 \times (P / T^2)\delta T$$

$$C_n^2(z) = \left\langle \delta n^2(x, y, z) \right\rangle_{x,y}$$

Light propagation through the turbulent atmosphere

- Index variations

$$C_n^2(z) = \left\langle \delta n^2(x,y,z) \right\rangle_{x,y}$$

- Total optical path variation

$$\phi(\mathbf{x}) = \left(\frac{2\pi}{\lambda}\right) \int_0^\infty \delta n(x,y,z)\,dz$$

- Wavefront aberration statistics: Structure Function D_ϕ

$$D_\phi(r) = \left\langle [\phi(\mathbf{x}) - \phi(\mathbf{x}+\mathbf{r})]^2 \right\rangle = 6.88 (r/r_0)^{-5/3}$$

Image Formation

- Field at the pupil plane

$$E(u) = A(u)\exp(i\phi(u))$$

- Field at the focal plane

$$F(\theta) = \frac{1}{\lambda}\int E(u)\exp(i2\pi u\cdot\theta/\lambda)du$$

- Average PSF at the focal plane

$$\langle PSF(\theta)\rangle = \left\langle |F(\theta)|^2 \right\rangle$$

$$\frac{1}{\lambda^2}\iint A(u)A(u+r)\langle\exp(i(\phi(u)-\phi(u+r)))\rangle\exp(-i2\pi r\cdot\theta/\lambda)du dr$$

Image formation (continued)

$$\langle PSF(\theta)\rangle = \left\langle \left|F(\theta)\right|^2 \right\rangle$$

$$\frac{1}{\lambda^2}\iint \underbrace{A(u)A(u+r)}_{\text{MTF of Pupil}}\underbrace{\langle \exp(i(\phi(u)-\phi(u+r)))\rangle}\exp(-i2\pi r\cdot\theta/\lambda)\,du\,dr$$

MTF of Pupil

$$\langle PSF(\theta)\rangle = \frac{A_0}{\lambda^2}\int B_0(r)\underbrace{\exp\left(-\frac{1}{2}D_\phi(r)\right)}_{B_A(r)}\exp(-i2\pi r\cdot\theta/\lambda)\,dr$$

MTF of Atmosphere

- <u>Strehl</u>: PSF(0) / PSF(0) $|_{\phi=0}$

Maximize Strehl ⇔ Minimize mean square wavefront error

(i.e. $S = B_A(0) \sim \exp\{-1/2\ D_\phi\}$, so make D_ϕ small)

Statistical characteristics of atmospheric wavefronts

Transverse correlation distance

$$r_0 = \left[0.423 \left(\frac{2\pi}{\lambda} \right)^2 \int_0^\infty C_n^2(z)\,dz \right]^{-3/5}$$

- Depends on λ
- Typical: r_0 = 20 cm at λ = 0.5 μ

Correlation angle

$$\theta_0 = \left[2.905 \left(\frac{2\pi}{\lambda} \right)^2 \int_0^\infty C_n^2(z)\, z^{5/3}\,dz \right]^{-3/5}$$

- Typical: θ_0 = 4 arcsec at λ = 0.5 μ
- Mean height of turbulence: $h_0 = r_0/\theta$
- h0 = 8.2 km

Correlation time

$$D_\phi(\tau) = \left\langle \left[\phi(t) - \phi(t+\tau) \right]^2 \right\rangle = \left(\frac{t}{\tau_0} \right)^{5/3}$$

$$\tau_0 = \left[2.91 \left(\frac{2\pi}{\lambda} \right)^2 \int_0^\infty C_n^2(z)\, v(z)^{3/5}\,dz \right]^{-3/5}$$

- Typical: τ_0 = 3 ms at λ = 0.5 μ
- Mean wind velocity: $v_0 = 0.314\, r_0/\tau_0$
- v_0 ~ 20 m/s

Atmospheric AO requirements

- Enough actuators to fit the wavefront
  - Actuator spacing $d \sim r_0$
- Fast enough update rate to keep up with the atmosphere
  - Temporal bandwidth $\tau_{CL} \sim \tau_0$
- Guidestar nearby science target
  - Isoplanatic patch: $\theta < \theta_0$
- Enough light from the guidestar to measure the wavefront accurately

Application Note

- One can consider any random wavefront ϕ
  - Optical fabrication or alignment errors
  - Calibration errors
  - Time-variable figure errors
  - …
- Just plug in 2nd order statistical moments to characterize imaging perfomance

Technologies for Atmospheric Adaptive Optics

Example: the Lick Observatory Adaptive Optics System

Lick Laser Guidestar Adaptive Optics System

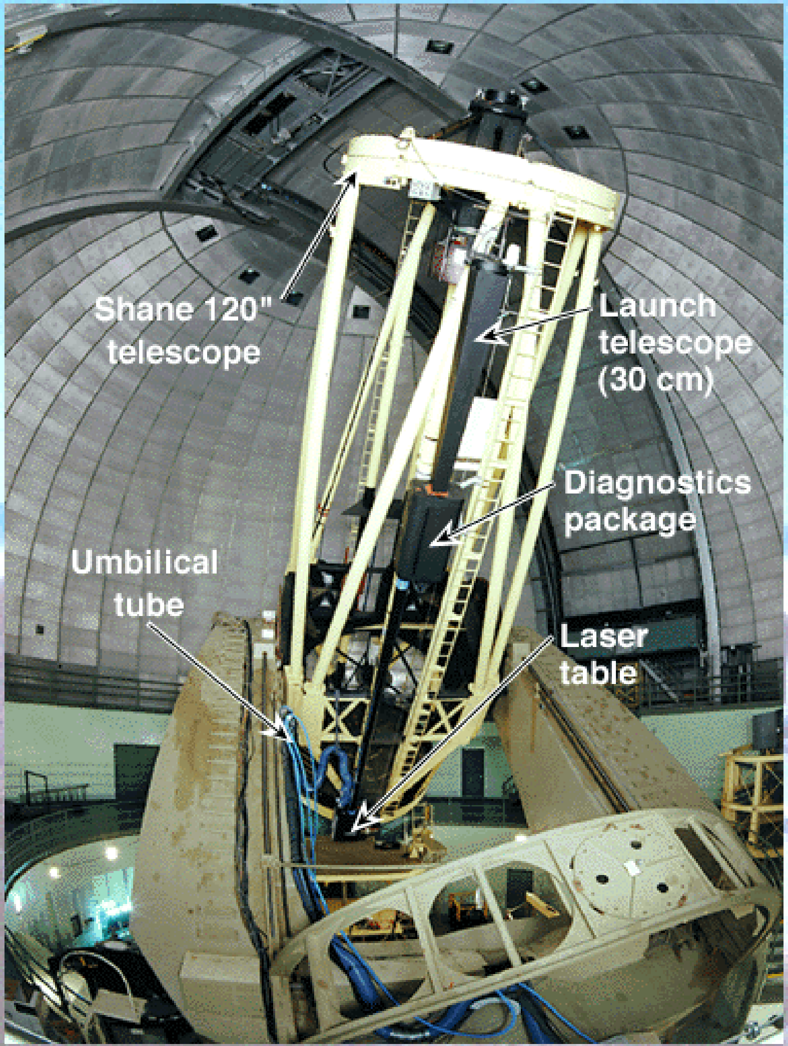

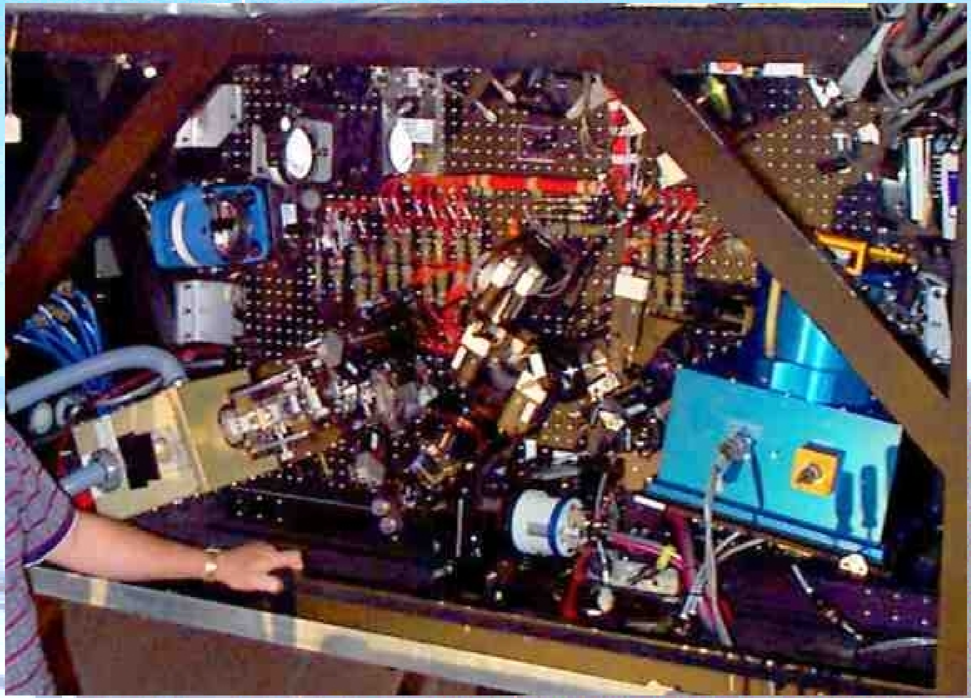

Schematic of astronomical adaptive optics system

- **Deformable mirror is optically conjugate to telescope primary mirror.**

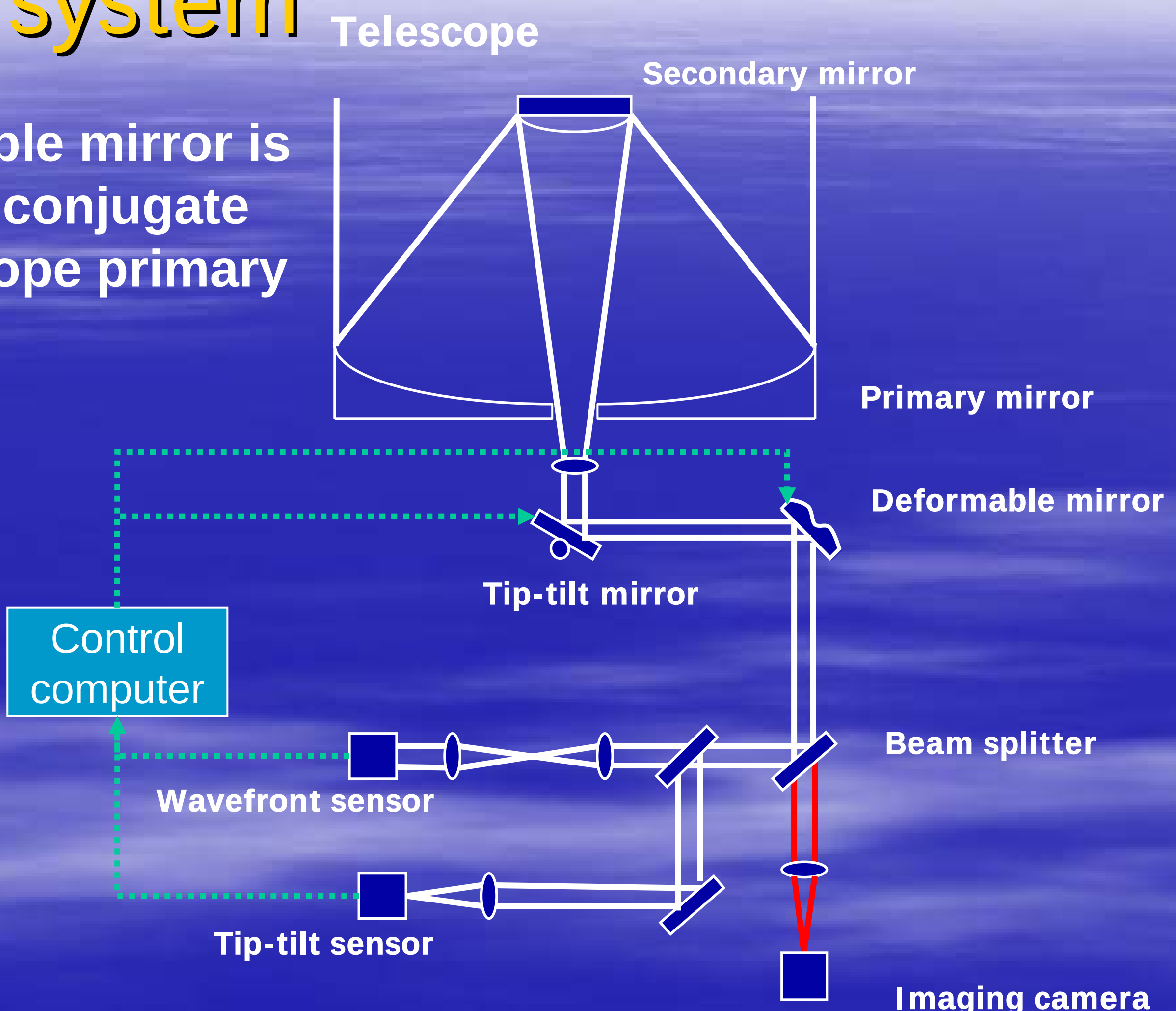

Lick AO System

3 m primary

0.8 m secondary

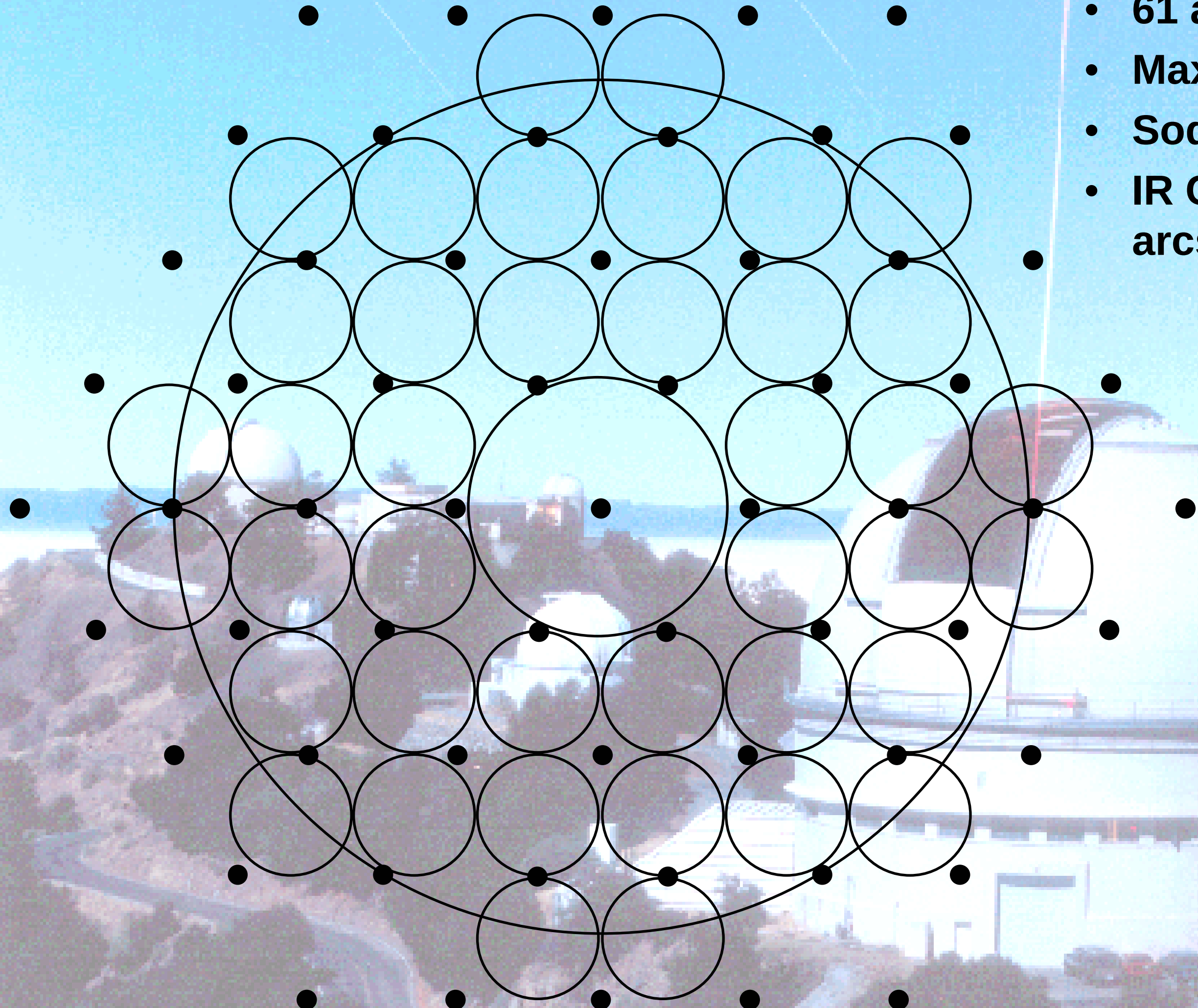

- 40 subabertures, d=43cm
- 61 actuators, hex grid, d_a=50cm
- Max sample rate: 500 Hz
- Sodium layer LGS
- IR Cam: 256^2 HgCdTe, 0.076 arcsec/pixel (Nyquist in K)

The laser produces an artificial star in the mesospheric Sodium layer

A small spot is important:

- Laser beam quality (M^2)
- Launch telescope aperture d_p matched to r_0 of atmosphere
- Translates to wavefront measurement accuracy

$$\sigma_{\substack{\text{wavefront}\\ \text{measurement}}} = (\text{spot size}) \times \frac{1}{\text{SNR}}$$

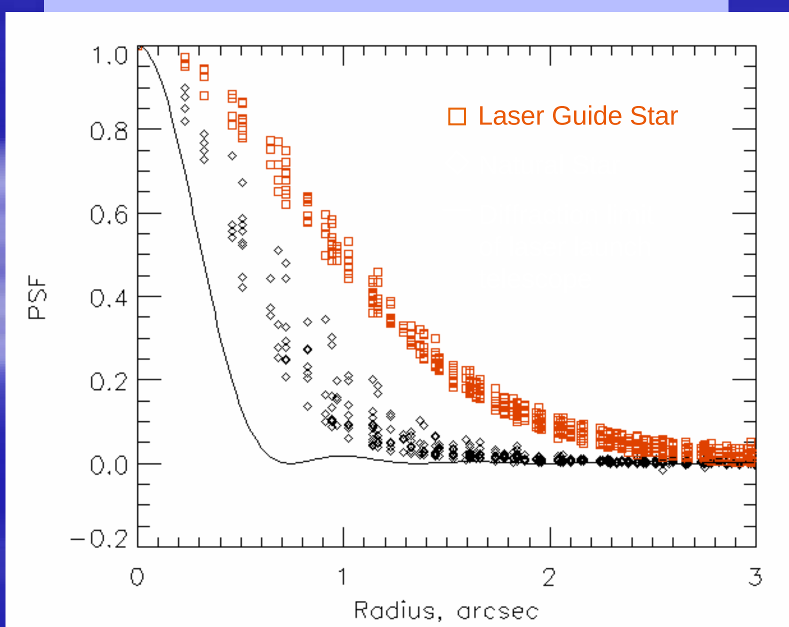

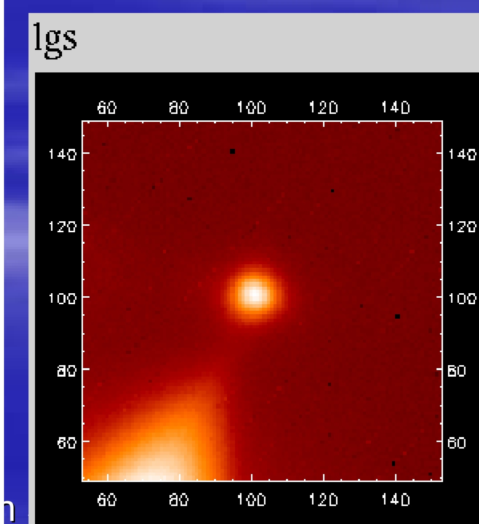

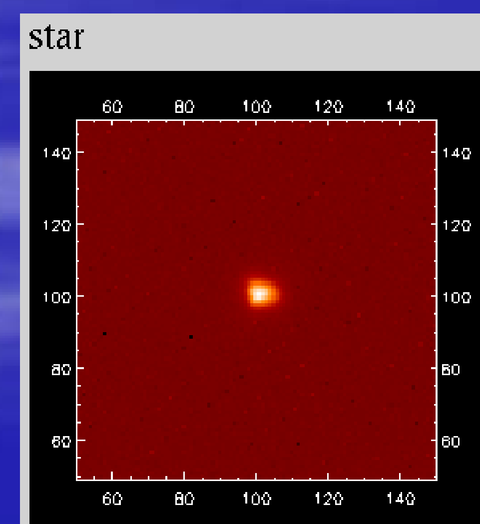

Measuring the wavefront

Overview of wavefront sensing

- Measure phase by measuring intensity variations
- Difference between various wavefront sensor schemes is the way in which phase differences are turned into intensity differences
- General block diagram:

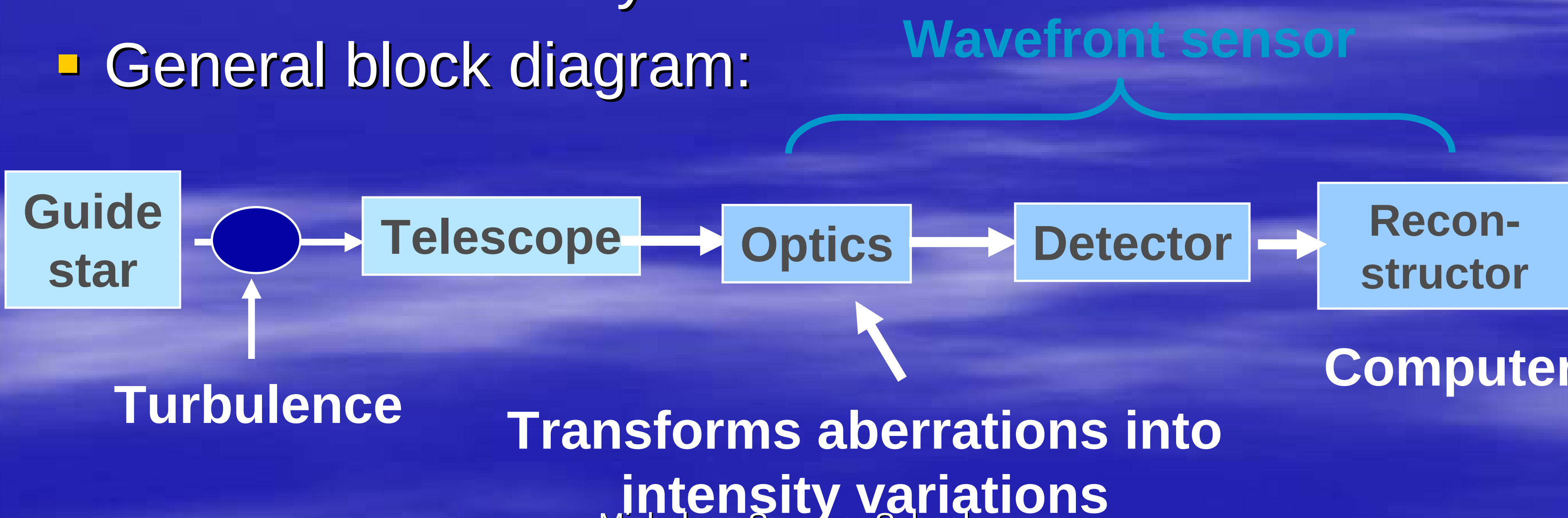

How to use intensity to measure phase?

- Irradiance transport equation: *A* is complex field amplitude.
  - (Teague, 1982, JOSA 72, 1199)

$$\text{Let } A(x,y,z) = \left[I(x,y,z)\right]^{1/2} \exp\left[ik\phi(x,y,z)\right]$$

- Follow *I(x,y,z)* as it propagates along the z axis (paraxial ray approximation: small angle w.r.t. z)

$$\frac{\partial I}{\partial z} = -\nabla I \bullet \nabla\phi - I\nabla^2\phi$$

Wavefront curvature

Wavefront tilt

Types of wavefront sensors

- “Direct” in pupil plane: split pupil up into subapertures in some way, then use intensity in each subaperture to deduce phase of wavefront. Sub-categories:
  - Slope sensing: Shack-Hartmann, shearing interferometer, pyramid sensing
  - Curvature sensing
  - Interferometric
- “Indirect” in focal plane: wavefront properties are deduced from whole-aperture intensity measurements made at or near the focal plane. Iterative methods - take a lot of time.
  - Image sharpening, multidither
  - Phase diversity

How to reconstruct wavefront from measurements of local "tilt"

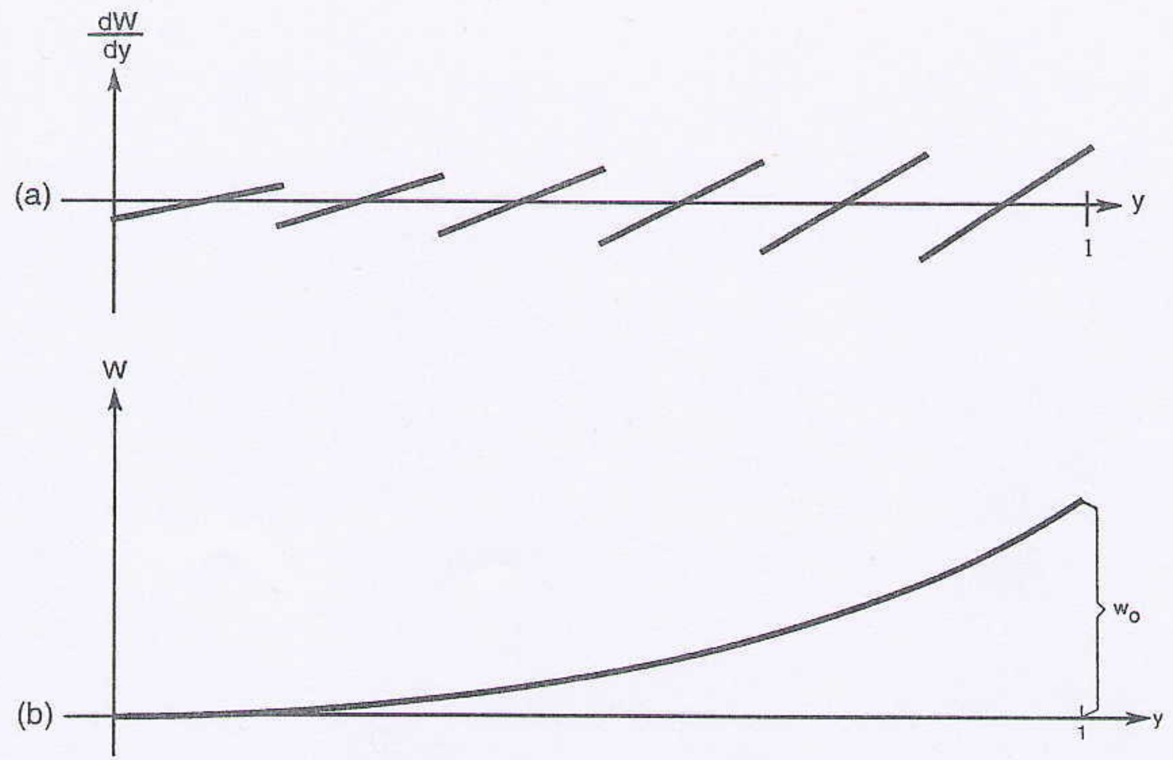

Figure 7 (a) Local tilt as a function of sampling location in pupil; (b) reconstructed wavefront estimate.

Shack-Hartmann wavefront sensor concept - measure subaperture tilts

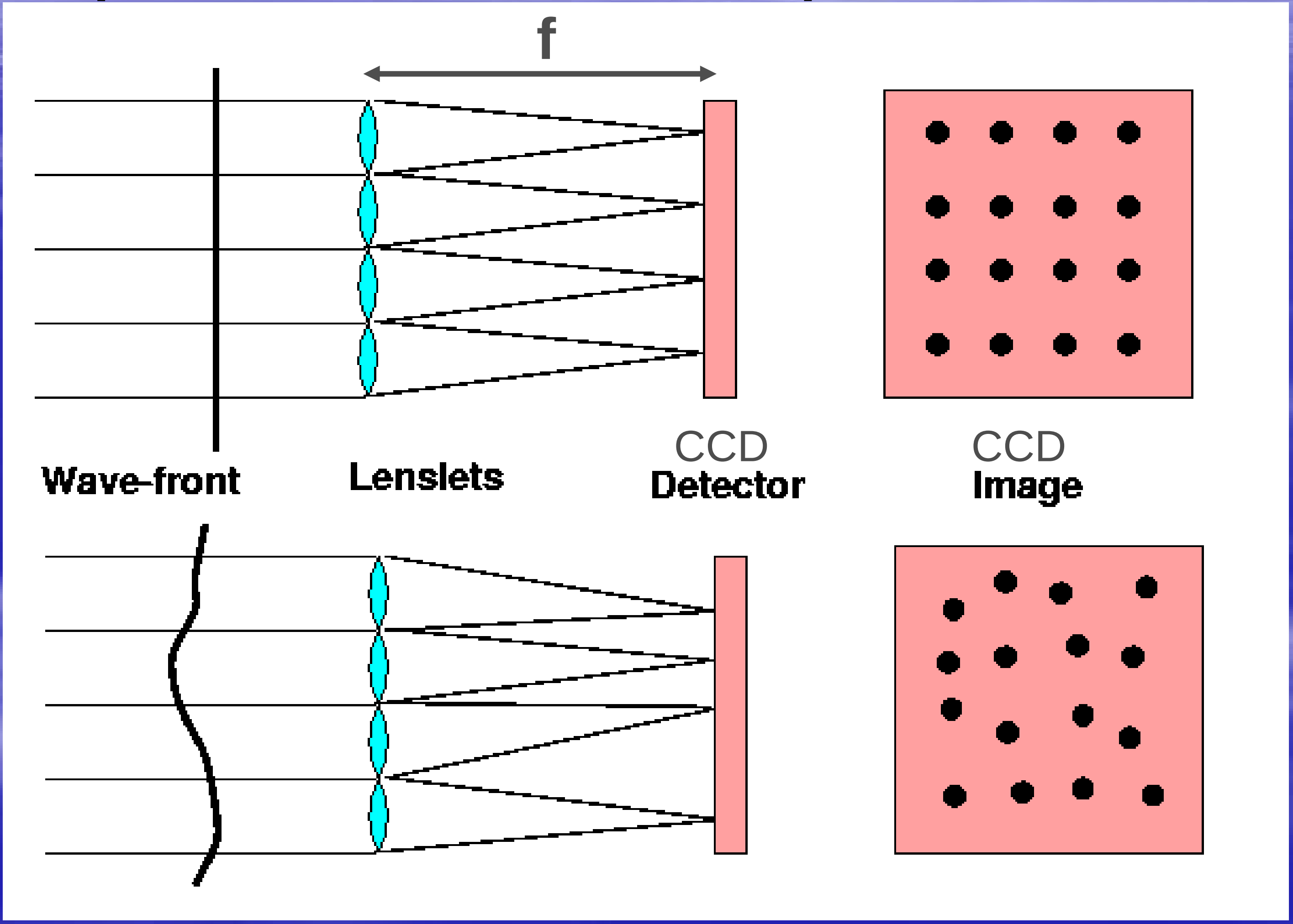

Example: Hartmann test of one Keck segment (static)

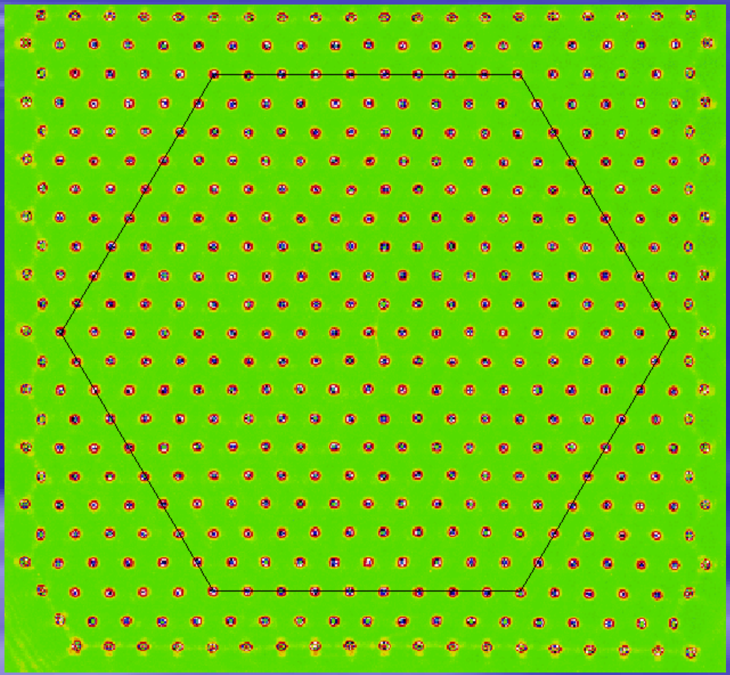

Reference flat wavefront

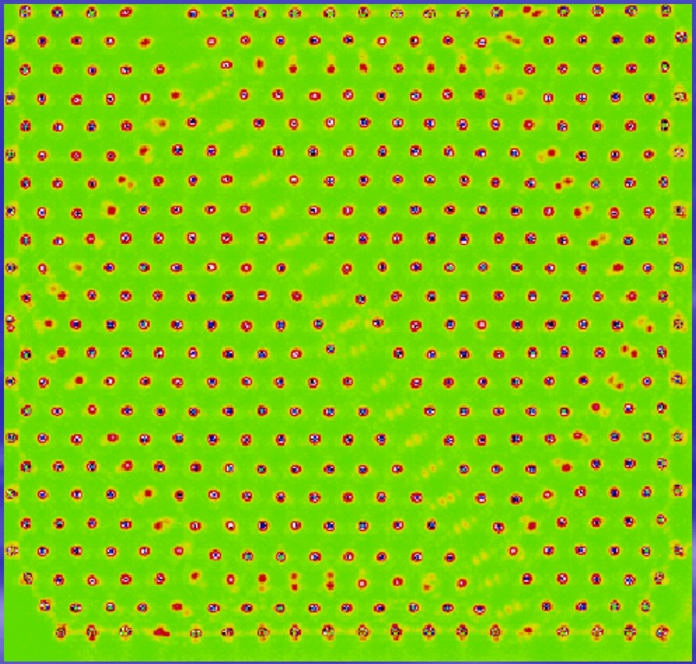

Measured wavefront

Gary Chanan, UCI

Resulting displacement of centroids

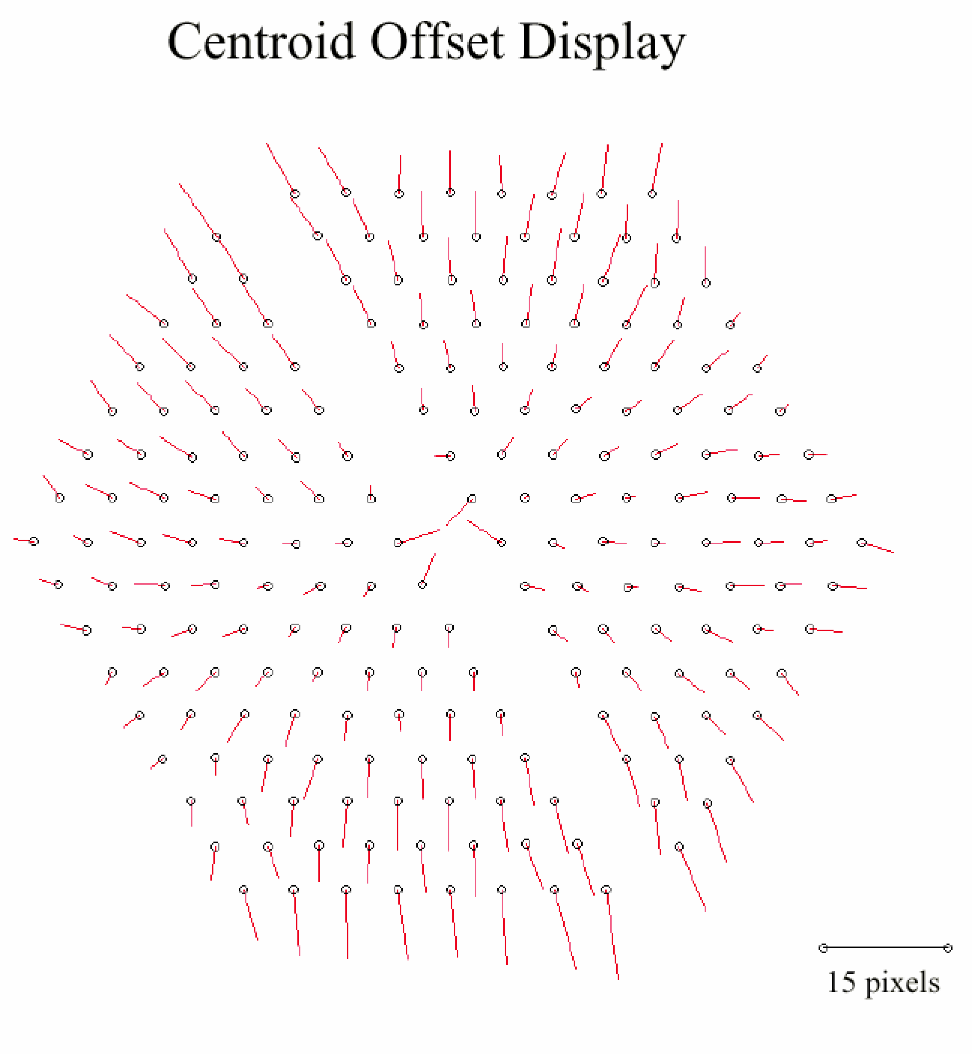

- Definition of centroid

$$\bar{x} \equiv \frac{\int\int I(x,y)\, x\, dxdy}{\int\int I(x,y)\, dxdy}$$

$$\bar{y} \equiv \frac{\int\int I(x,y)\, y\, dxdy}{\int\int I(x,y)\, dxdy}$$

- Each arrow represents an offset proportional to its length

How to measure distance a spot has moved on CCD? "Quad cell formula"

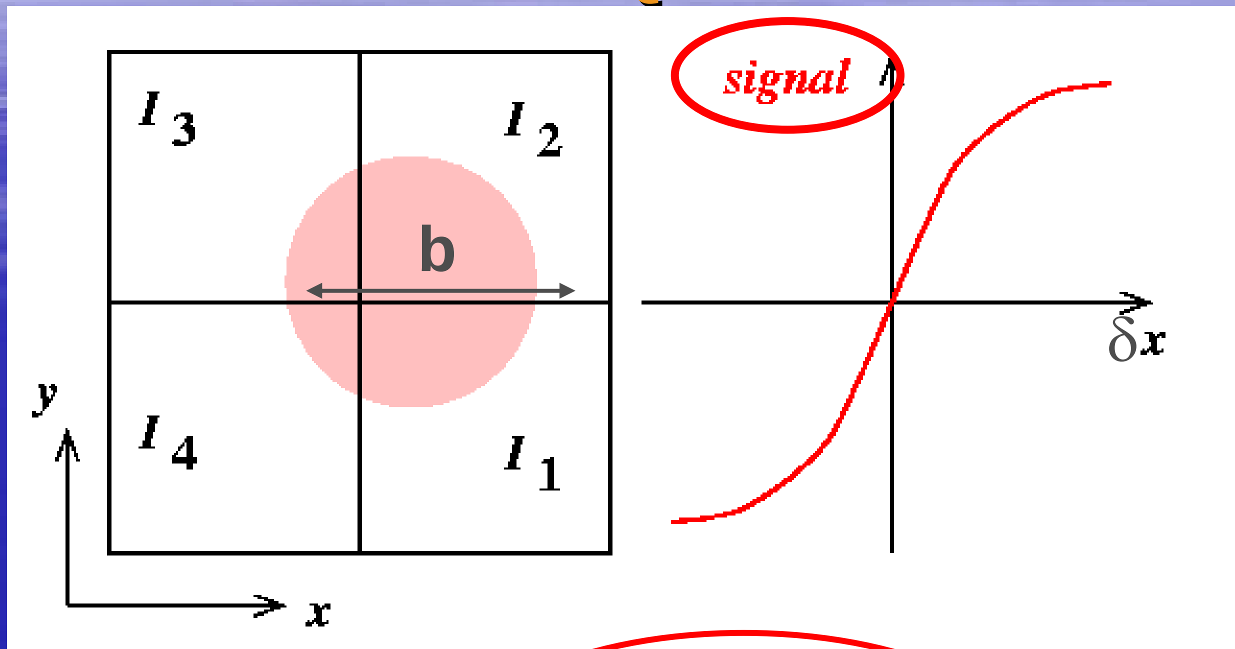

$$\delta_x \cong \frac{b}{2}\left[\frac{(I_2+I_1)-(I_3+I_4)}{(I_1+I_2+I_3+I_4)}\right]$$

$$\delta_y \cong \frac{b}{2}\left[\frac{(I_3+I_2)-(I_4+I_1)}{(I_1+I_2+I_3+I_4)}\right]$$

Disadvantage: "gain" depends on spot size b which can vary during the night

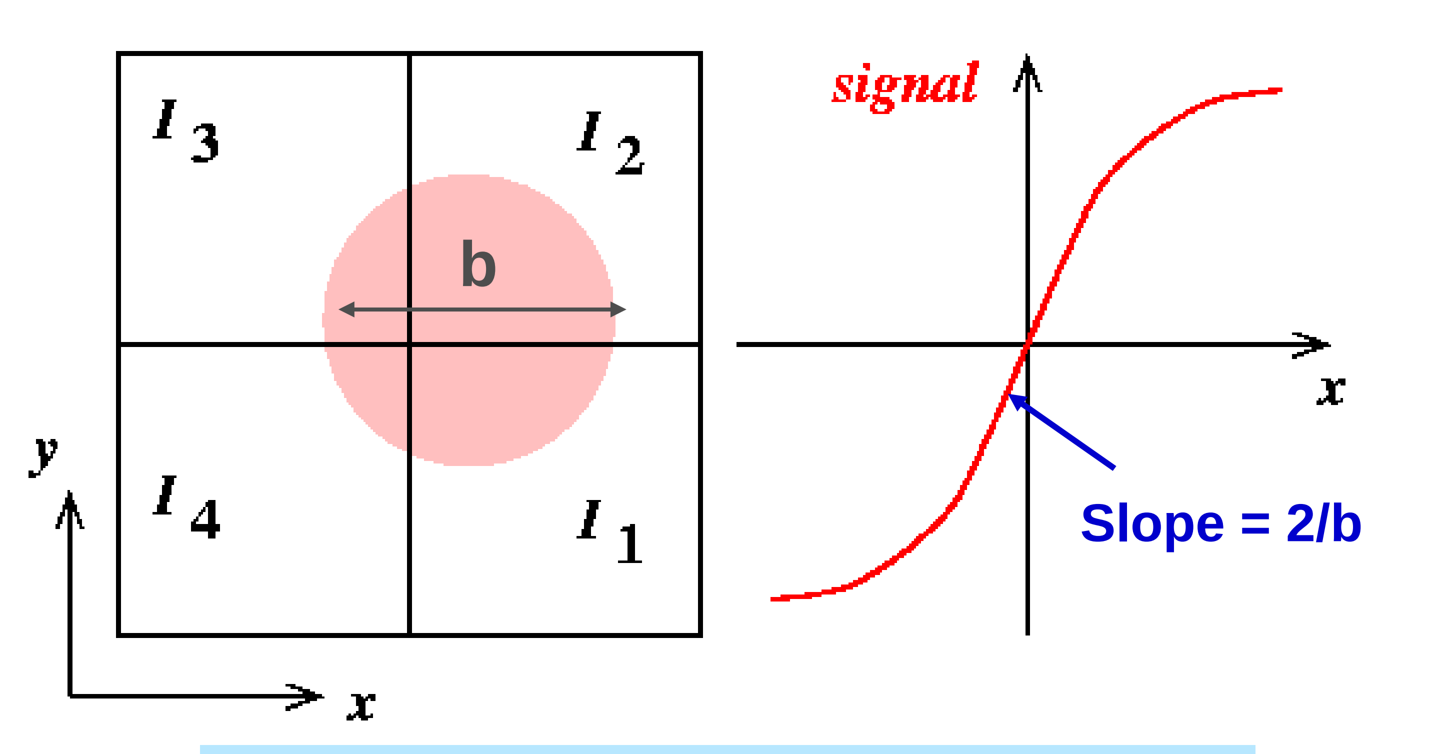

$$\delta_{x,y} = \frac{b}{2}\frac{(difference\ of\ I\ 's)}{(sum\ of\ I\ 's)}$$

Another disadvantage: signal becomes nonlinear for large angular deviations

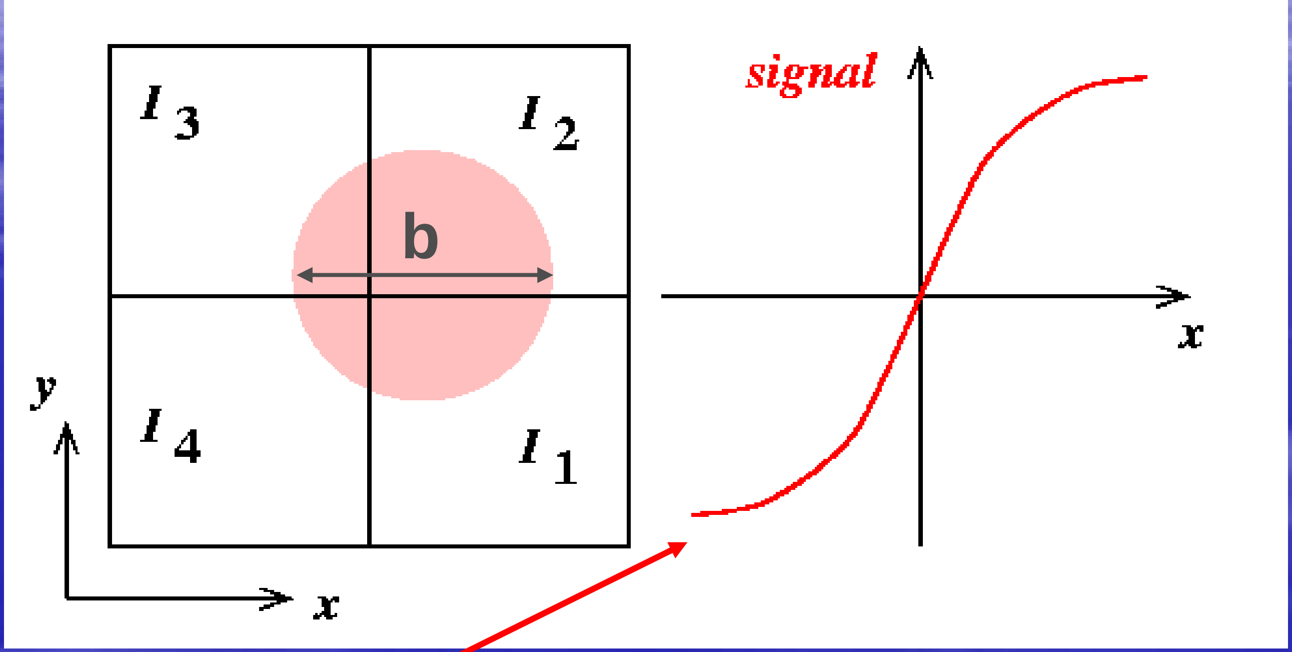

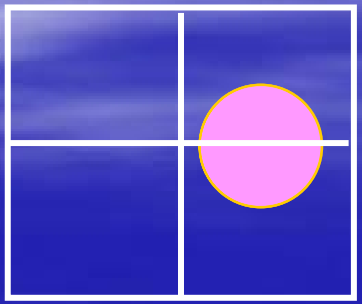

"Rollover" corresponds to spot being entirely outside of 2 quadrants

General expression for signal to noise ratio of a pixelated detector

- S = flux of detected photoelectrons / subap
- n_{pix} = number of detector pixels per subaperture
- R = read noise in electrons per pixel
- Then the signal to noise ratio in a subaperture for fast CCD cameras is dominated by read noise, and

$$SNR \approx \frac{S t_{\mathrm{int}}}{\left(n_{pix} R^2 / t_{\mathrm{int}}\right)^{1/2}} = \frac{S\sqrt{t_{\mathrm{int}}}}{\sqrt{n_{pix}}\, R}$$

See McLean, "Electronic Imaging in Astronomy", Wiley, Sect. 10.9

Measurement error from Shack-Hartmann sensing

- Measurement error depends on size of spot as seen in a subaperture, θ_b , wavelength λ , subap size *d*, and signal-to-noise ratio SNR:

$$\sigma_{SNR} = \eta d \, \frac{\theta_b}{SNR} \approx \eta d \, \frac{\lambda / r_0}{SNR}$$

Trade-off between dynamic range and sensitivity of Shack-Hartmann WFS

- If spot is diffraction limited in a subaperture *d*, linear range of a quad cell (2x2 pixels) is limited to $\pm \lambda_{ref}/2d$ radian or a half-wave.
- Can increase dynamic range by enlarging the spot (e.g. by defocusing it).
- But uncertainty in calculating centroid $\propto$ width x $N_{ph}^{1/2}$ so centroid calculation will be less accurate.
- Alternative: use more than 2x2 pixels per subaperture. Decreases *SNR* if read noise per pixel is large (more pixels).

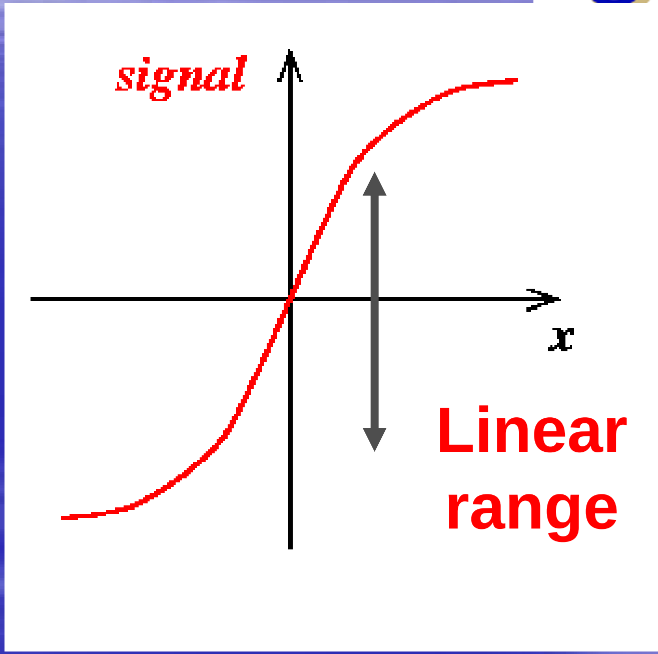

Curvature wavefront sensing

- F. Roddier, Applied Optics, 27, 1223- 1225, 1998

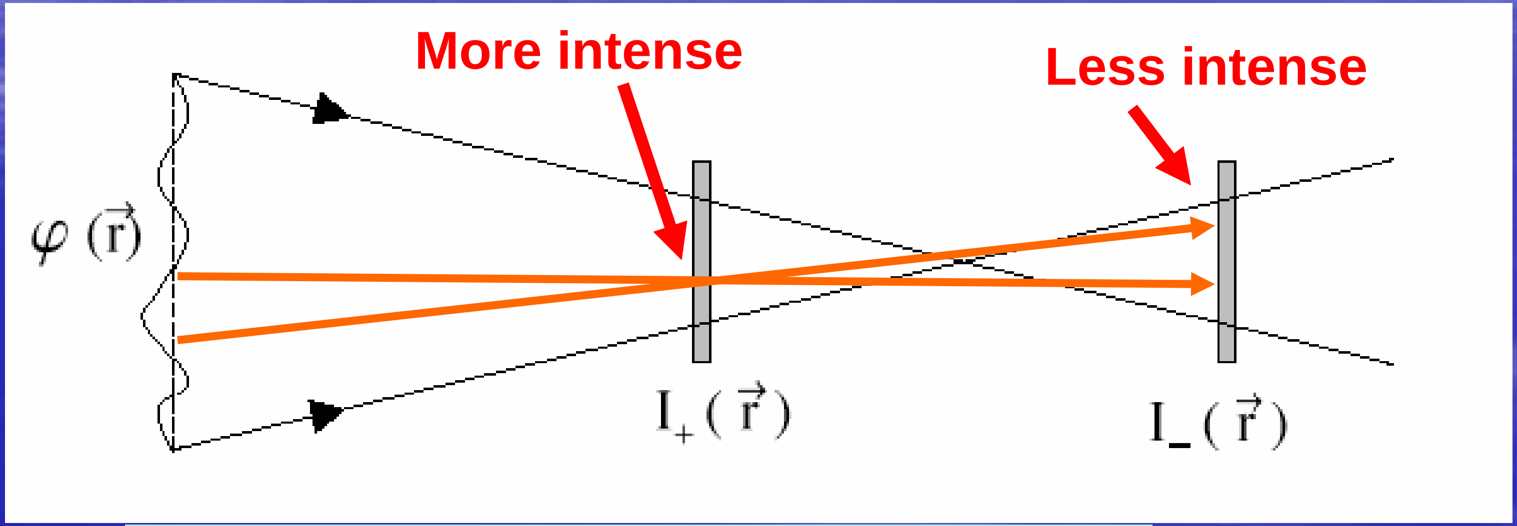

$$\frac{I_+ - I_-}{I_+ + I_-} \propto \nabla^2 \phi - \frac{\partial \phi}{\partial \vec{r}} \vec{\delta}_R$$

Normal derivative at boundary

Laplacian (curvature)

Wavefront sensor lenslet shapes are different for edge, middle of pupil

- Example: This is what wavefront tilt (which produces image motion) looks like on a curvature wavefront sensor
  - Constant I on inside
  - Excess I on right edge
  - Deficit on left edge

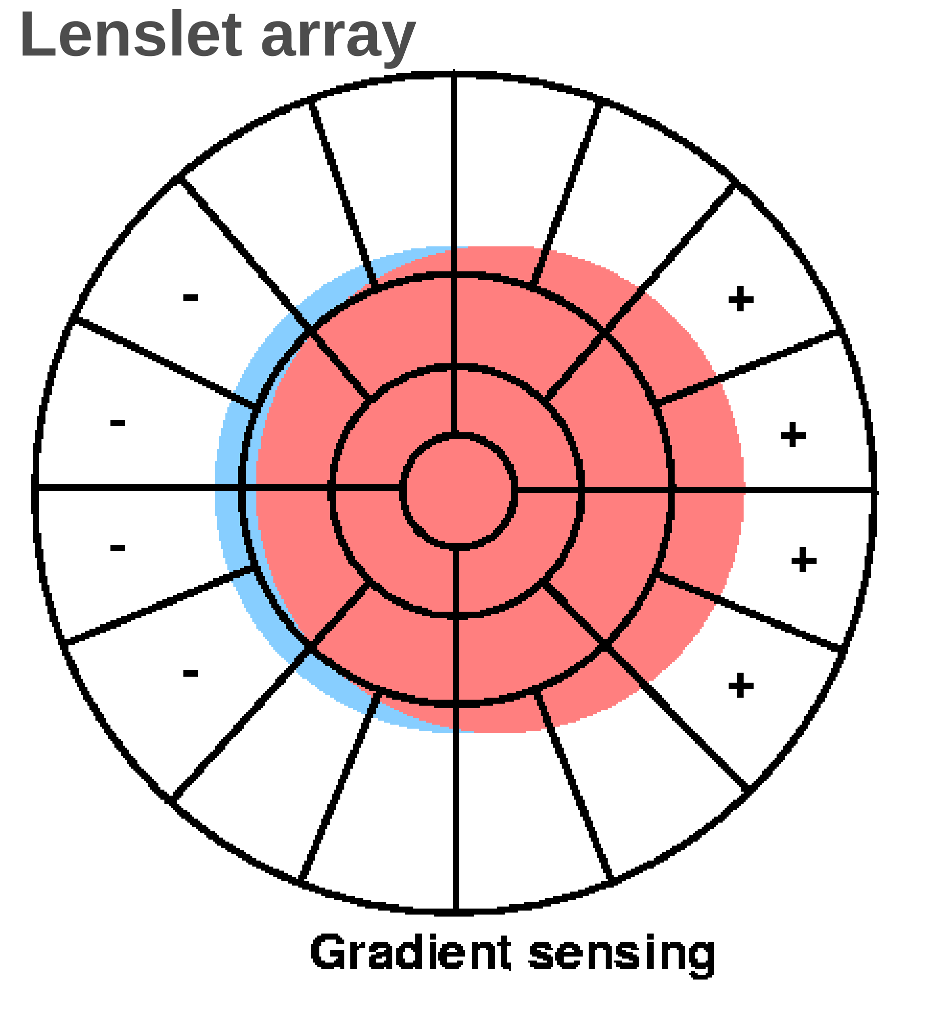

Simulation of curvature sensor response

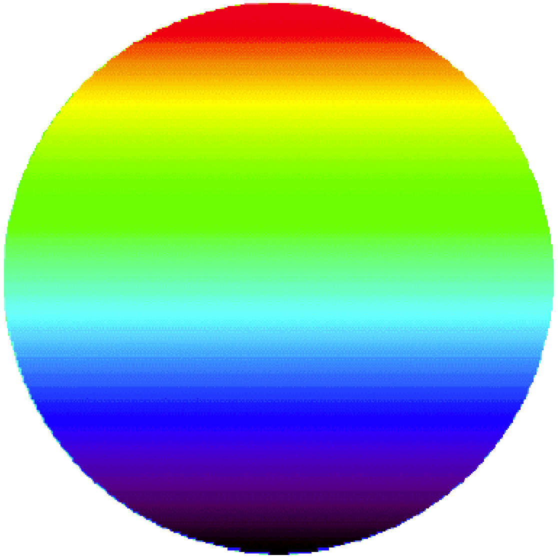

$Z_{1,-1}$

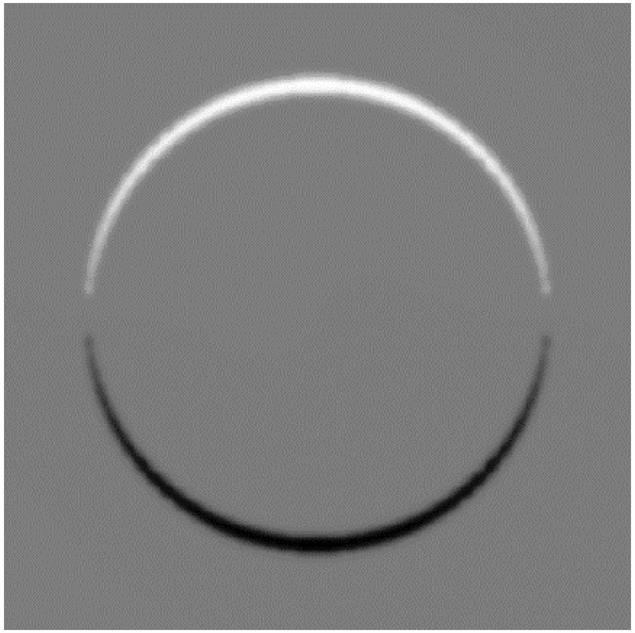

Difference Image

G. Chanan

Wavefront: pure tilt **Curvature sensor signal**

Curvature sensor signal for astigmatism

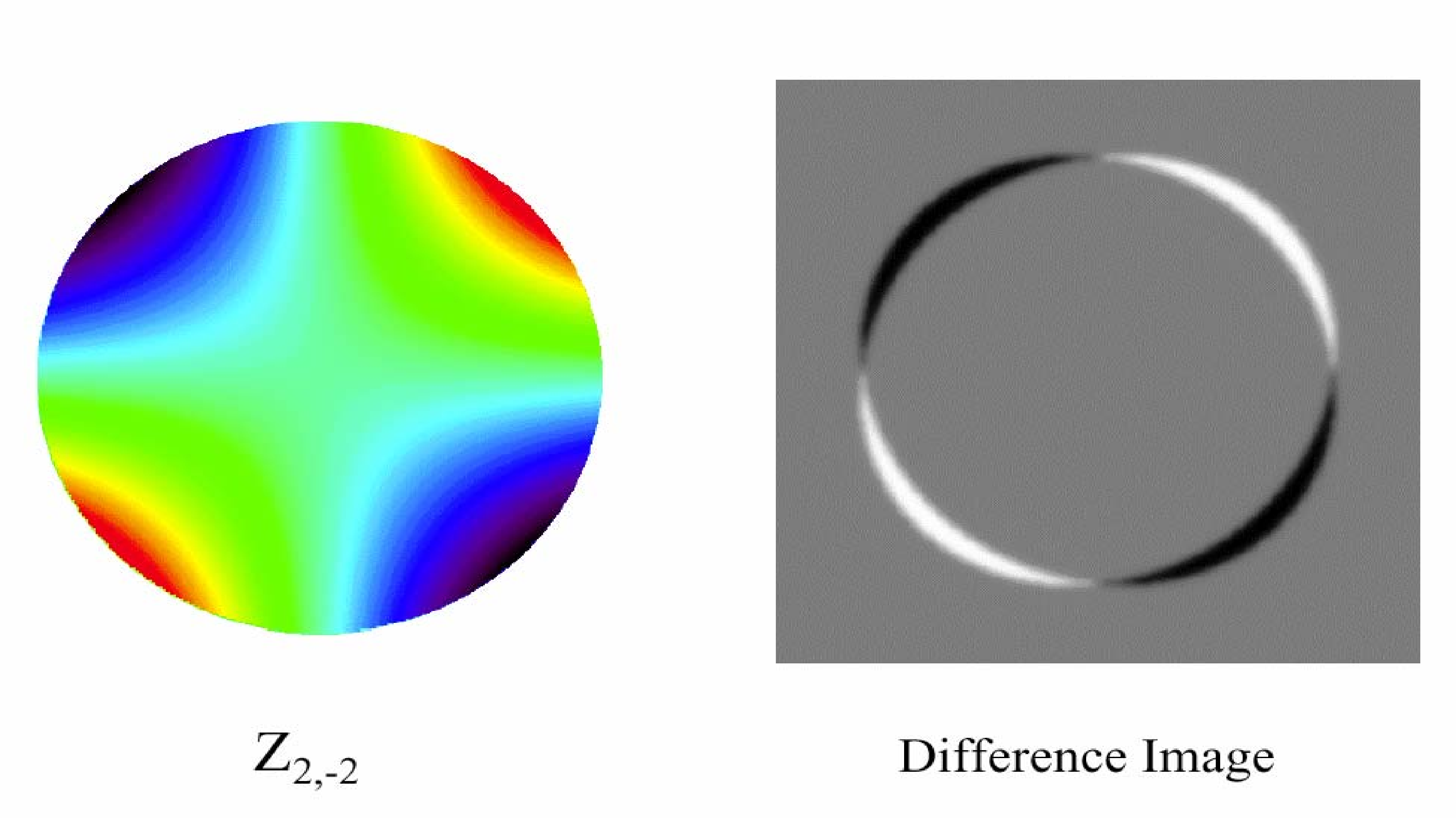

G. Chanan

Third order spherical aberration

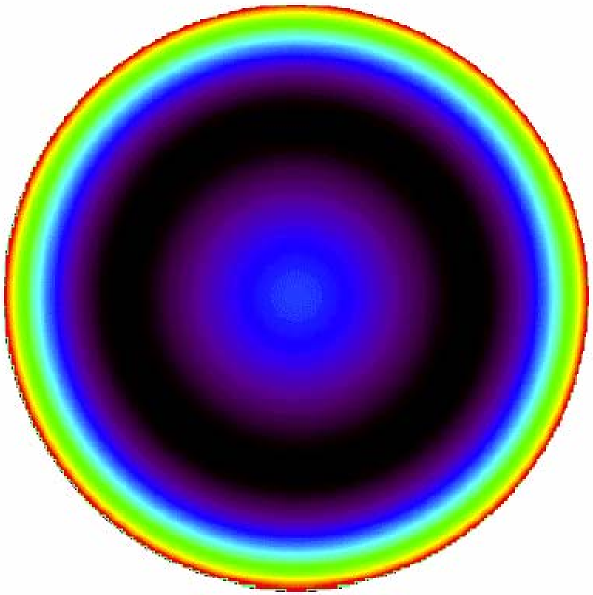

$Z_{4,0}$

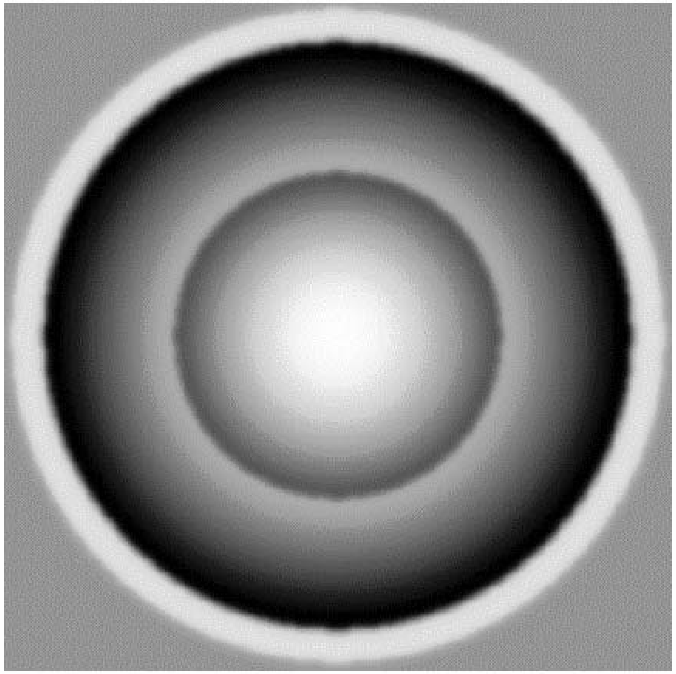

Difference Image

G. Chanan

Practical implementation of curvature sensing

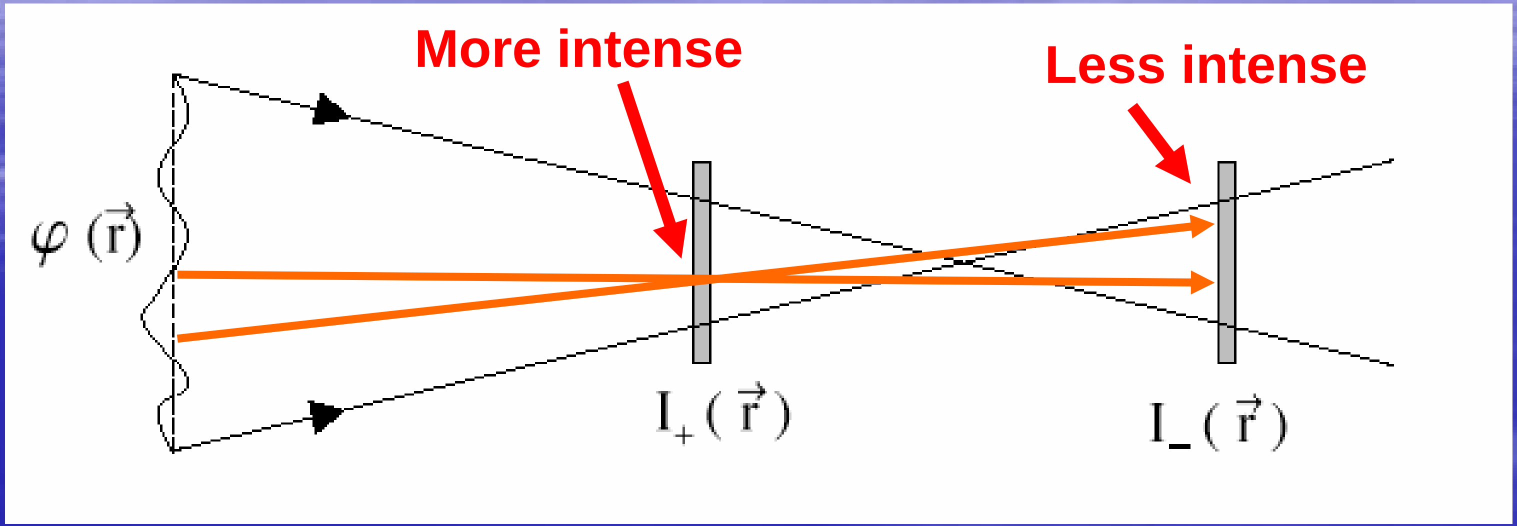

- Use oscillating membrane mirror (2 kHz!) to vibrate rapidly between I_+ and I_- extrafocal positions
- Measure intensity in each subaperture with an "avalanche photodiode" (only need one per subaperture!)
  – Detects individual photons, no read noise, QE ~ 60%
  – Can read out very fast with no noise penalty

Measurement error from curvature sensing

- Error of a single set of measurements is determined by photon statistics, since detector has no noise:

$$\sigma_{cs}^2 = \pi^2 \frac{1}{N_{ph}} \left(\frac{\theta_b d}{\lambda} \right)^2$$

where θ_b = apparent guide star size, λ = wavelength, d = subaperture diameter and N_{ph} is no. of photoelectrons per subaperture per sample period

- Error propagation when the wavefront is reconstructed numerically using a computer scales poorly with no. of subapertures N:
  – $(\text{Error})_{\text{curvature}} \propto N$, whereas $(\text{Error})_{\text{Shack-Hartmann}} \propto \log N$

Advantages and disadvantages of curvature sensing

- Advantages:
  - Lower noise $\Rightarrow$ can use fainter guide stars than S-H
  - Fast readout $\Rightarrow$ can run AO system faster
  - Can adjust amplitude of membrane mirror excursion as “seeing” conditions change. Affects sensitivity.
  - Well matched to bimorph deformable mirror (both solve Laplace’s equation), so less computation.
  - Curvature systems appear to be less expensive.
- Disadvantages:
  - Avalanche photodiodes can fail if too much light falls on them. They are bulky and expensive. Hard to use a large number of them.

Shearing Interferometry

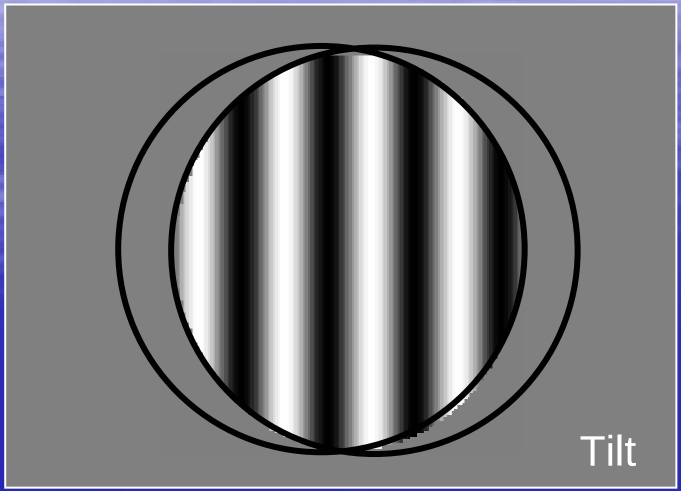

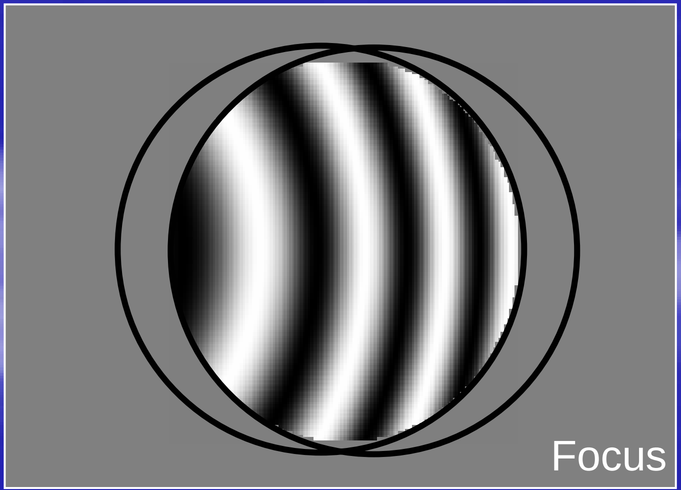

- Interfere a wavefront with itself, slightly shifted in x, y
- Intensity $1+\sin(d\phi/dx)$, $1+\sin(d\phi/dy)$
- Reconstruct phase from slope by solving

$$\mathbf{s} = \nabla \phi$$

$$\nabla \cdot \mathbf{s} = \nabla^2 \phi$$

Shearing Interferometry

- Advantages
  - Can adjust shear as seeing conditions change
  - Guide star extent affects fringe visibility, more easily subtracted to normalize slope sensitivity
  - Information/photon roughly the same as Hartmann sensor, noise propagator the same
- Disadvantages
  - Phase unwrapping issue
  - More difficult to implement, splitting can be inefficient

Pyramid Sensing

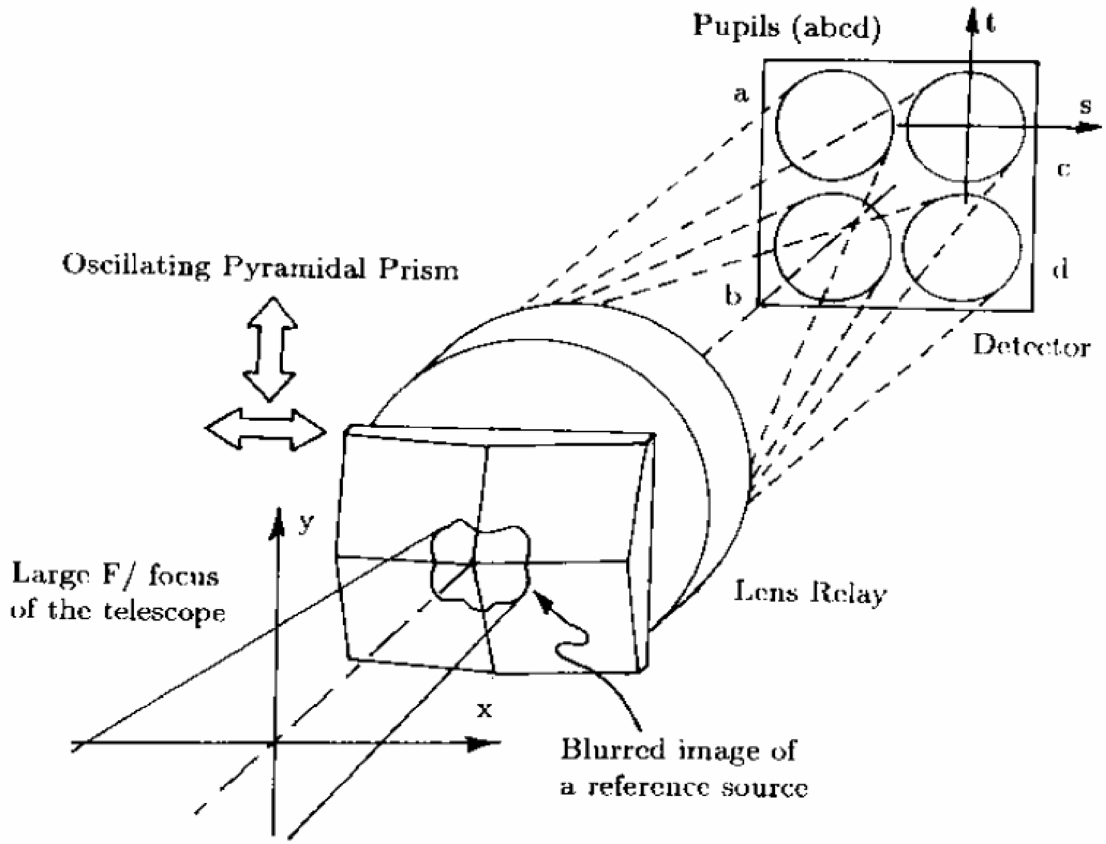

Figure 1. The overall layout of the wavefront sensor concept described in the text.

Pyramid Sensing

- Essentially a “transposed” Hartmann sensor

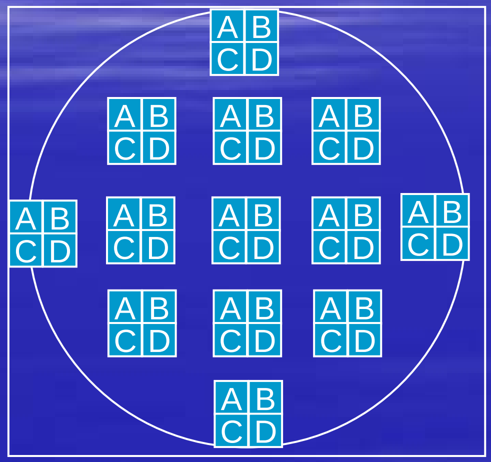

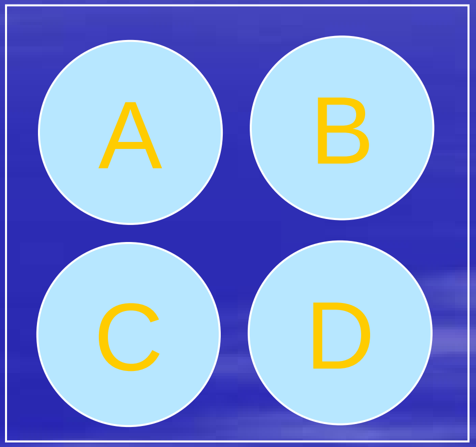

- Hartmann and Pyramid are variations of the knife-edge test
  - Pyramid: the knife edge is the pyramid edge
  - Hartmann: the knife edge is the pixel boundary

Direct Phase Detection

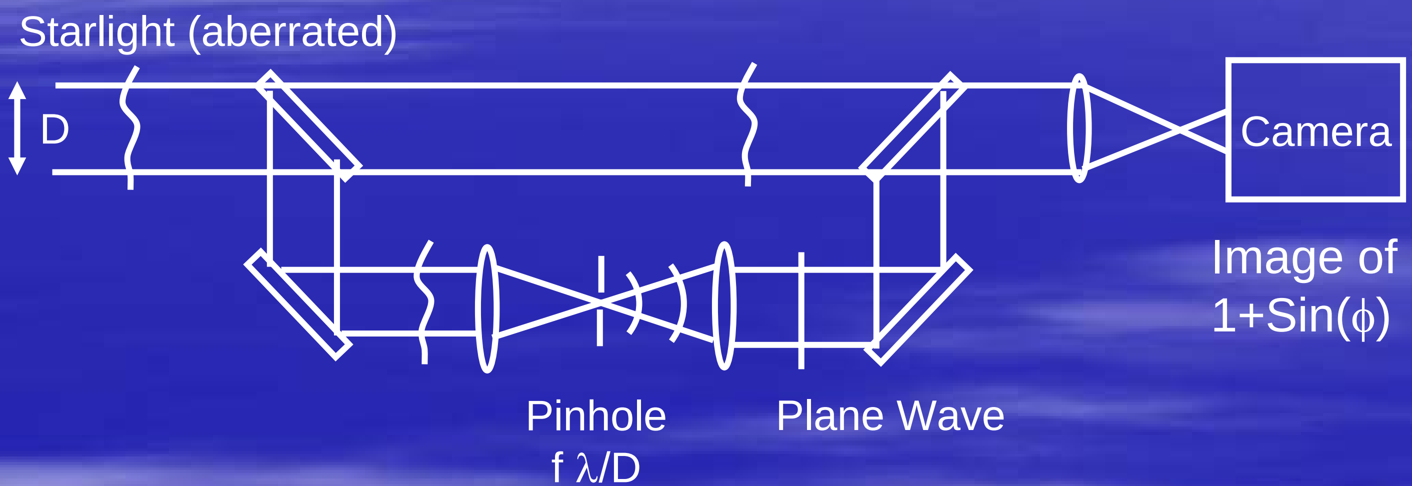

Mach-Zhender Point Diffraction Interferometer

Controlling the wavefront

Overview of wavefront correction

- Divide pupil into regions of size r_0 , do “best fit” to wavefront
- Several types of deformable mirror (DM), each has its own characteristic “fitting error”

$$\sigma_{fitting}^2 = a_F \, (d / r_0)^{5/3} \ \mathrm{rad}^2$$

- Other requirements: dynamic range (the farthest excursion the mirror surface can take), frequency response, influence function of actuators, surface quality (smoothness), hysteresis, power dissipation

Typical role of actuators

- Actuators are glued to back of glass mirror
- When you apply a voltage (PZT) or a magnetic field (PMN) to the actuator, it expands or contracts in length, thereby pushing or pulling on the mirror

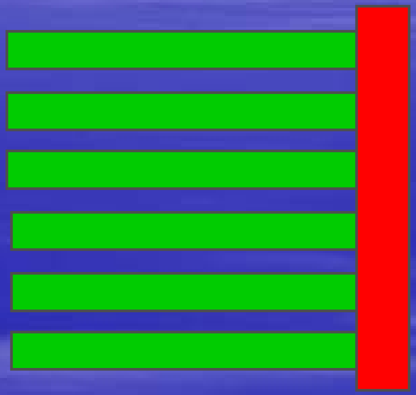

Types of actuator: Piezoelectric

- PZT (lead zirconate titanate) gets longer or shorter when you apply V
- Stack of PZT ceramic disks with integral electrodes
- Typically 150 Volts $\Rightarrow \Delta x \sim 10$ microns
- 10-20% hysteresis:

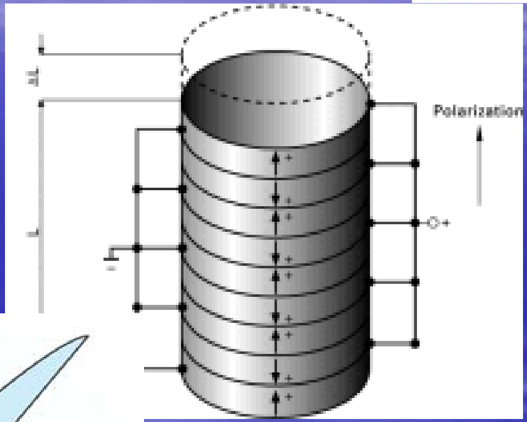

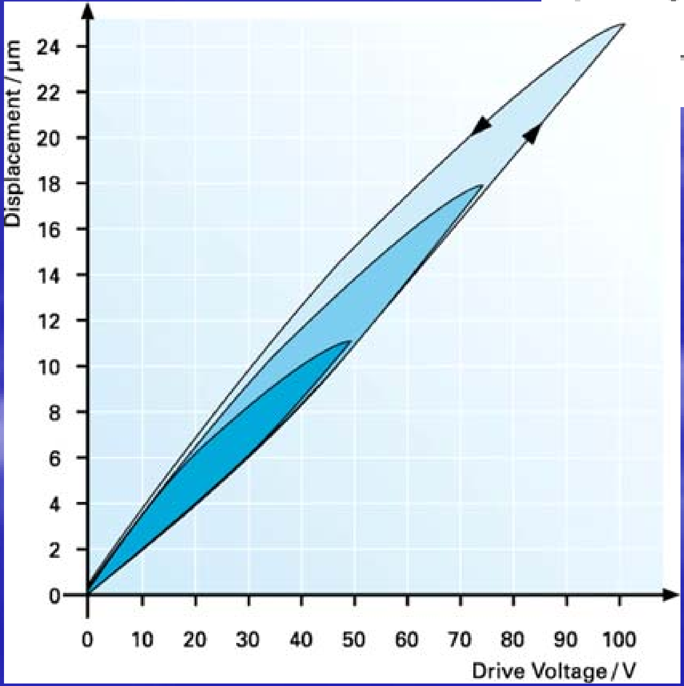

Types of actuator: PMN

- Lead magnesium niobate (PMN)
- Magnetistrictive:
  - Material gets longer or shorter in response to an applied magnetic field
- Can “push” and “pull” if a magnetic bias is applied
- Somewhat higher hysteresis than PZT: ~ 20%

In general, hysteresis is bad for AO

- Want response to voltage to be linear and one-to-one
- With hysteresis, response is nonlinear and non-unique

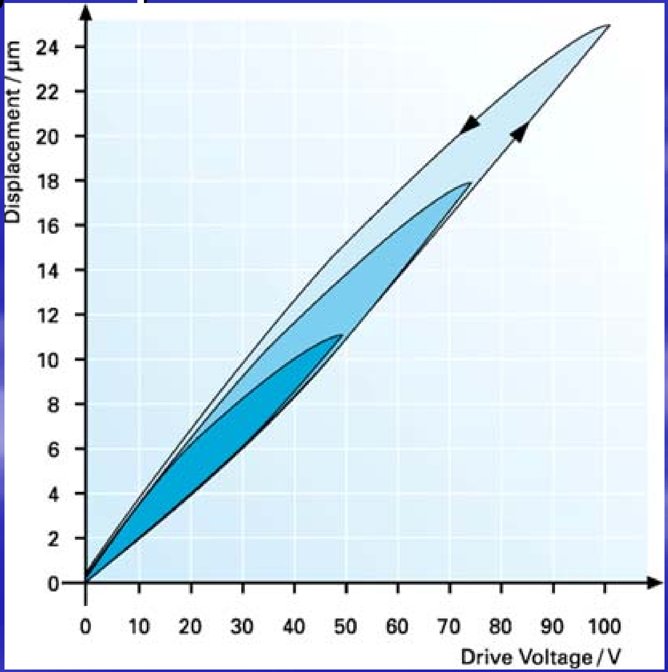

DM requirements

- Dynamic range: stroke (total up and down range)
  - Typical "stroke" for astronomy ± several microns. For vision science up to 10 microns
- Temporal frequency response:
  - DM must respond faster than coherence time τ_0
- Influence function of actuators:
  - Shape of mirror surface when you push just one actuator (like Greens' function)
  - Can optimize your AO system with a particular influence function, but pretty forgiving

DM requirements, part 2

- Surface quality:
  - Small-scale bumps can't be corrected by AO
- Hysteresis of actuators:
  - Want actuators to go back to same position when you apply the same voltage
- Power dissipation:
  - Don't want too much resistive loss in actuators, because heat is bad ("seeing", distorts mirror)
  - Lower voltage is better (easier to use, less power dissipation)

Types of deformable mirrors: large

- Segmented
  - Made of separate segments with small gaps
  - Each segment has 1 - 3 actuators and can correct:
    - Piston only (in and out), or
    - Piston plus tip-tilt (three degrees of freedom)
- "Continuous face-sheet"
  - Thin glass sheet with actuators glued to the back
  - Zonal (square actuator pattern), or
  - Modal (sections of annulae, as in curvature sensing)
- Bimorph
  - 2 piezoelectric wafers bonded together with array of electrodes between them. Front surface acts as mirror.

Types of deformable mirrors: small

- Liquid crystal spatial light modulators
  - Technology similar to LCDs for computer screens
  - Applied voltage orients long thin molecules, changes index of refraction
  - Response time too slow?
- MEMS (micro-electro-mechanical systems)
  - Fabricated using microfabrication methods of the integrated circuit industry
  - Many mirror configurations possible
  - Potential to be very inexpensive

Segmented deformable mirrors: concept

- Each actuator can move just in piston (in and out), or in piston plus tip-tilt (3 degrees of freedom)
- Fitting error:

  $\sigma_{fitting}^{2} = a_F \, (d/r_0)^{5/3}$

- Piston only: $a_F = 1.26$
- 3 degrees of freedom:

  $a_F = 0.18$

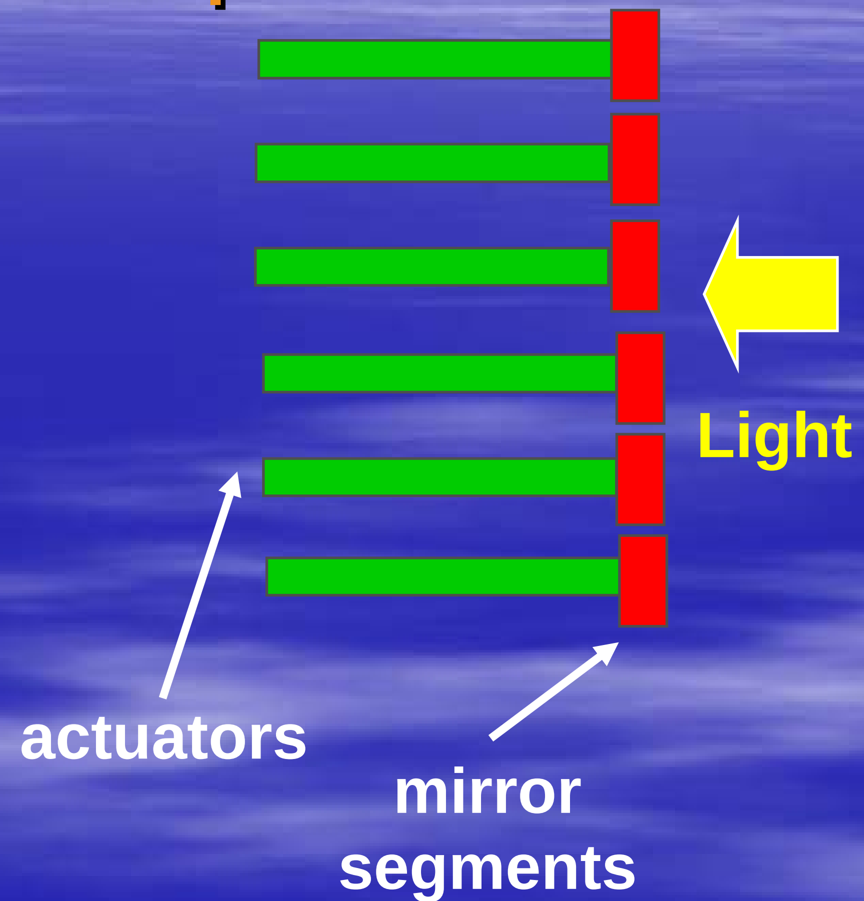

Segmented deformable mirrors: Example

- NAOMI (William Herschel Telescope, UK): 76 element segmented mirror
- Each square mirror is mounted on 3 piezos, each of which has a strain gauge
- Strain gauges provide independent measure of movement, are used to reduce hysteresis to below 1% (piezo actuators have ~10% hysteresis).

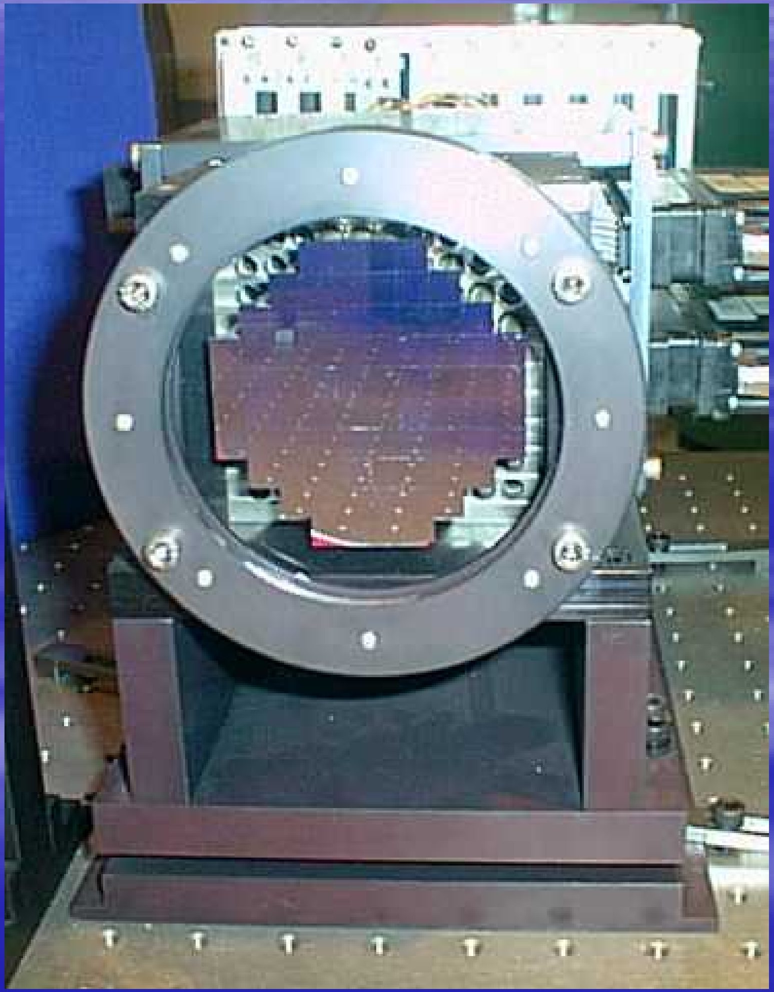

Largest segmented DM: Thermotrex

- 512 segments
- Each with 3 dof
- Overall diam. 22 cm

Built in early 1990's for military

Continuous face-sheet DMs: Design considerations

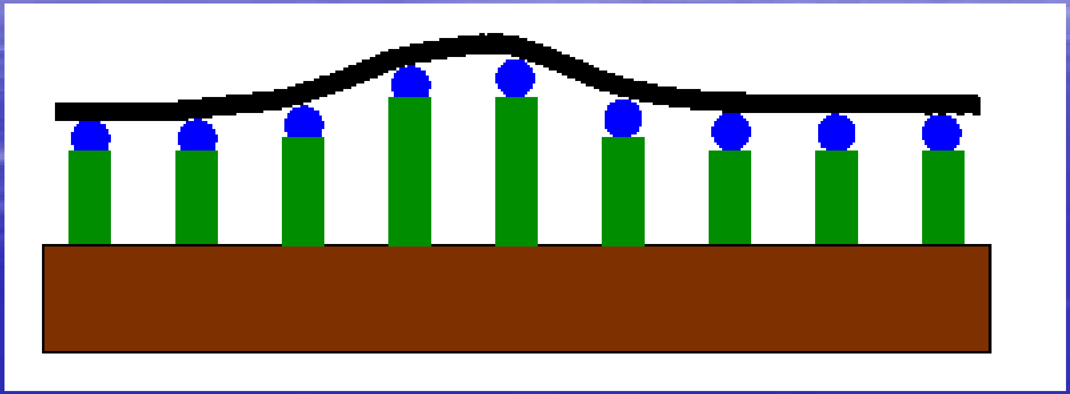

- Facesheet thickness must be large enough to maintain flatness during polishing, but low enough to deflect when pushed or pulled by actuators
- Thickness also determines “influence function”
  – Response of mirror shape to “push” by 1 actuator
- Actuators have to be stiff, so they won’t bend sideways as the mirror deflects

Continuous face-sheet DM's: Fitting error

$$\sigma_{fitting}^2 = a_F \, (d/r_0)^{5/3} \text{ rad}^2$$

where $a_F = 0.28$

Continuous face-sheet DM's: Xinetics product line

Front view of Xinetics DM (Keck)

349 degrees of freedom; 250 in use at any one time

(paper coasters)

Rear view of Xinetics 349 actuator DM used in Keck Telescope AO system

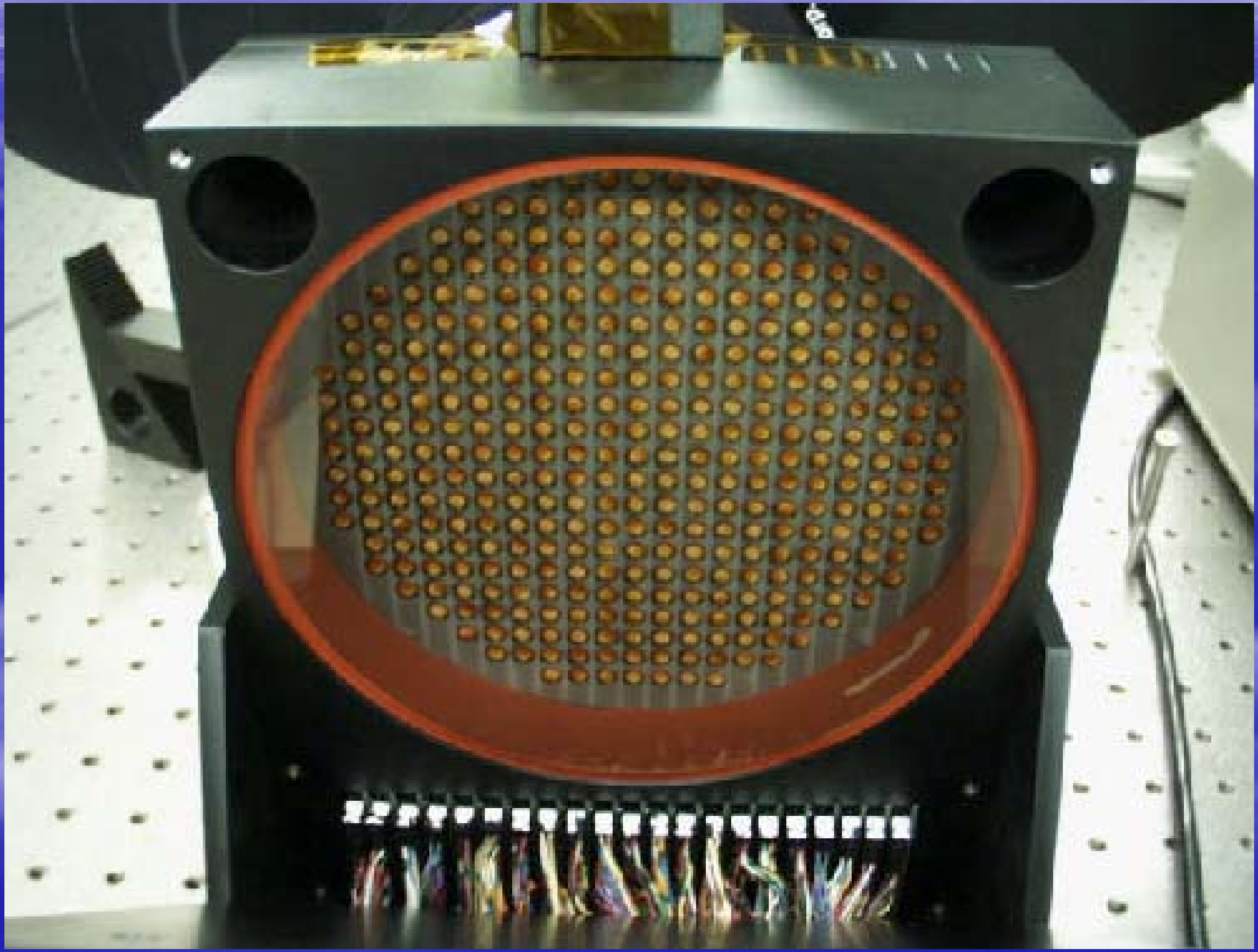

Influence functions for Xinetics DM

- Push on four actuators, measure deflection with an optical interferometer

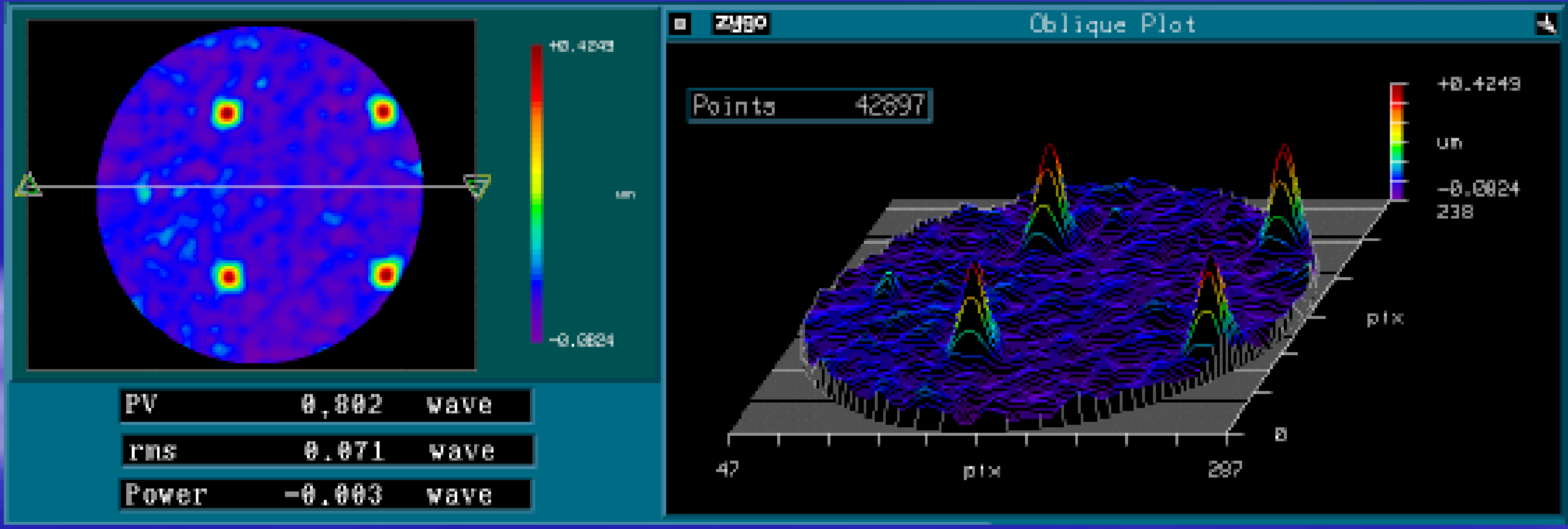

Bimorph mirrors

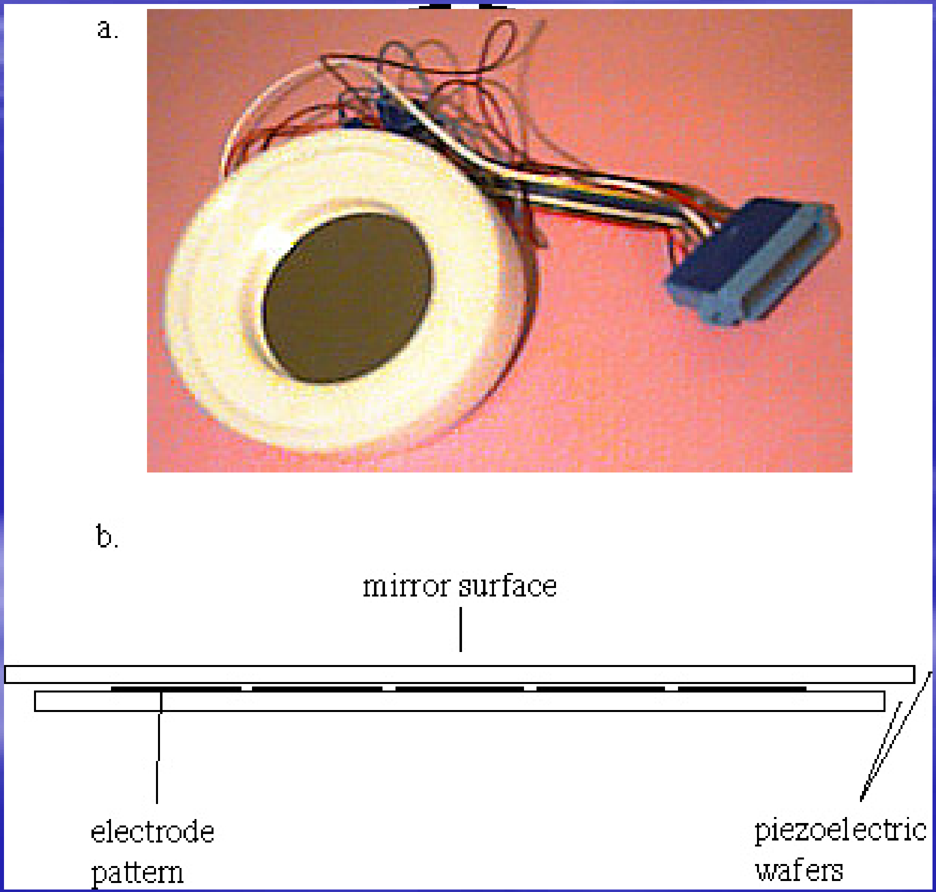

- Bimorph mirror made from 2 piezoelectric wafers with an electrode pattern between the two wafers to control deformation

- Front and back surfaces are electrically grounded.

- When V is applied, one wafer contracts as the other expands, inducing curvature

Bimorph mirrors well matched to curvature sensing AO systems

- Electrode pattern can be shaped to match subapertures in curvature sensor
- Mirror shape W(x,y) obeys Poisson Equation

$$\nabla^2\left(\nabla^2 W + AV\right) = 0$$

where $A = 8\, d_{31} / t^2$

d_{31} is the transverse piezo constant

t is the thickness

$V(x,y)$ is the voltage distribution

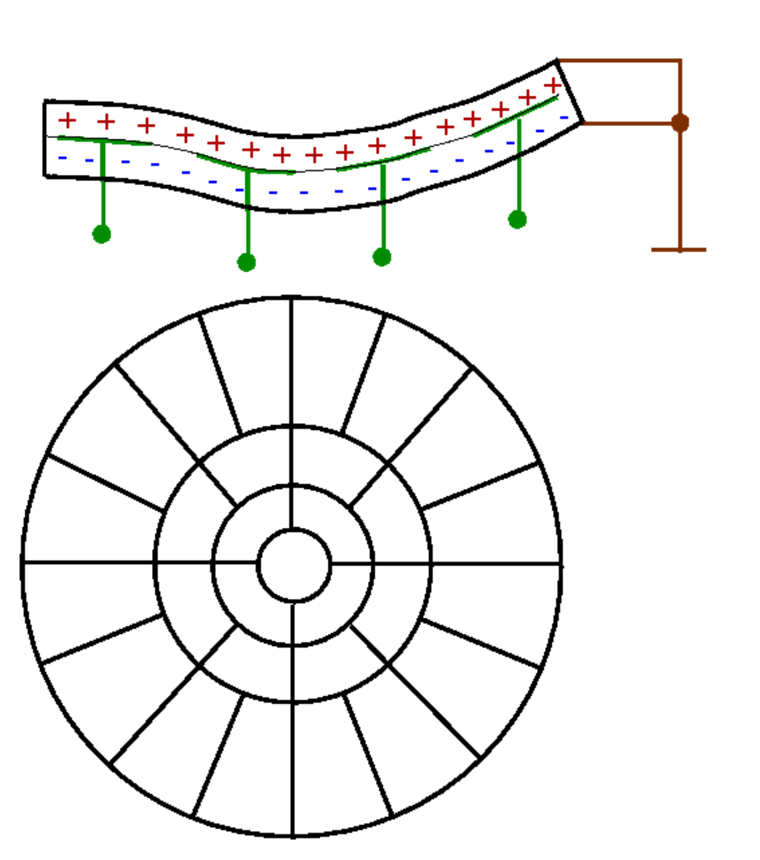

What are MEMs deformable mirrors?

A promising new class of deformable mirrors, called MEMs DMs, has emerged in the past few years.

Devices fabricated using semiconductor batch processing technology and low power electrostatic actuation.

Potential to be very inexpensive ($10/actuator instead of $1000/actuator)

MEMS: micro-electro-mechanical systems

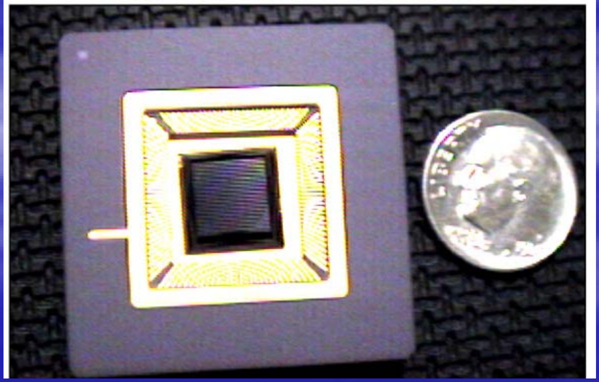

Boston University MEMS Concept

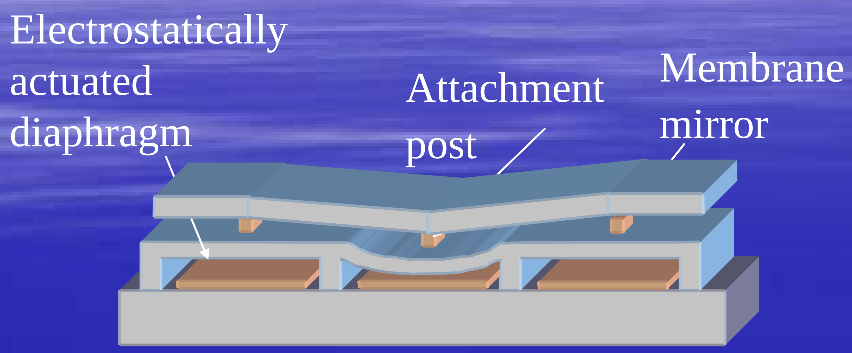

Continuous mirror

Boston University
Boston MicroMachines

- Fabrication: Silicon micromachining (structural silicon and sacrificial oxide)
- Actuation: Electrostatic parallel plates
- Currently testing 1000 actuator MEMS device

Some other MEMS DM concepts

Delft University (OKO)

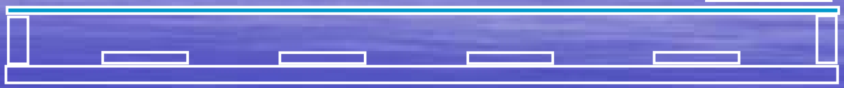

- Underlying electrode array
- Continuous membrane mirror

JPL, SY Tech., AFIT

- Surface micromachined, segmented
- Lenslet cover for improved fill factor

Boston University

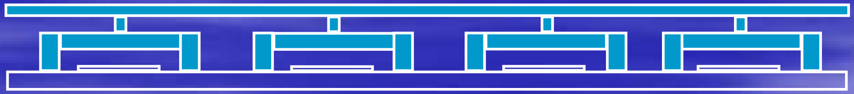

- Surface micromachined
- Continuous membrane mirror

Texas Instruments

- Surface micromachined
- Tip and tilt only

Narrow anchors reduce undesirable print-through in BU MEMS

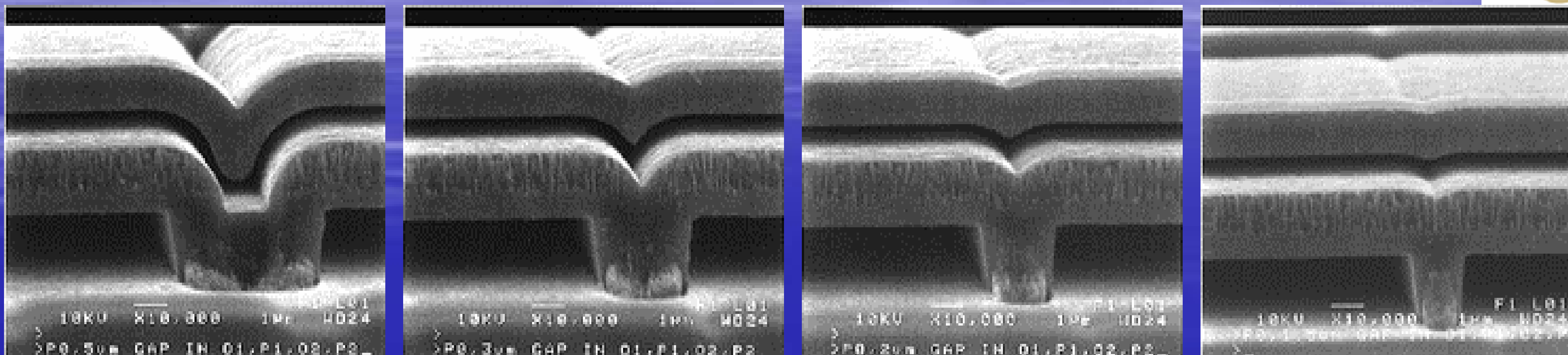

5µ 2.5µ 2µ 1.5µ

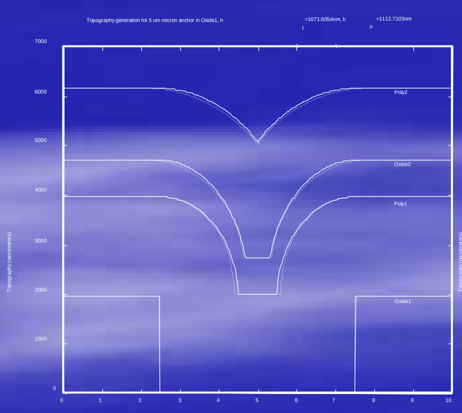

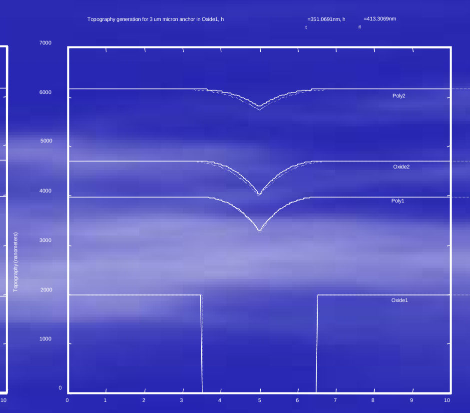

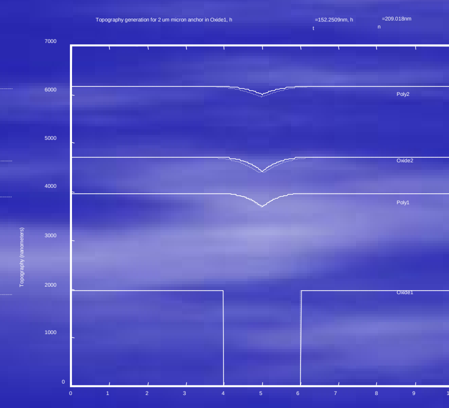

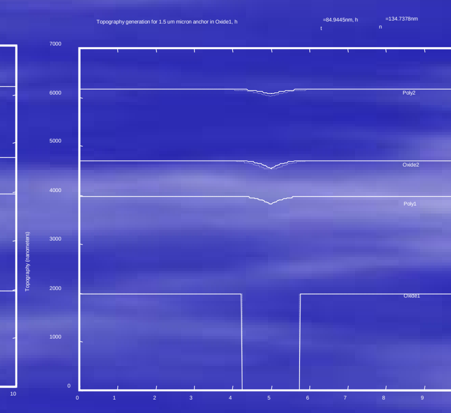

Influence functions for 100 actuator BU MEMS deformable mirrors

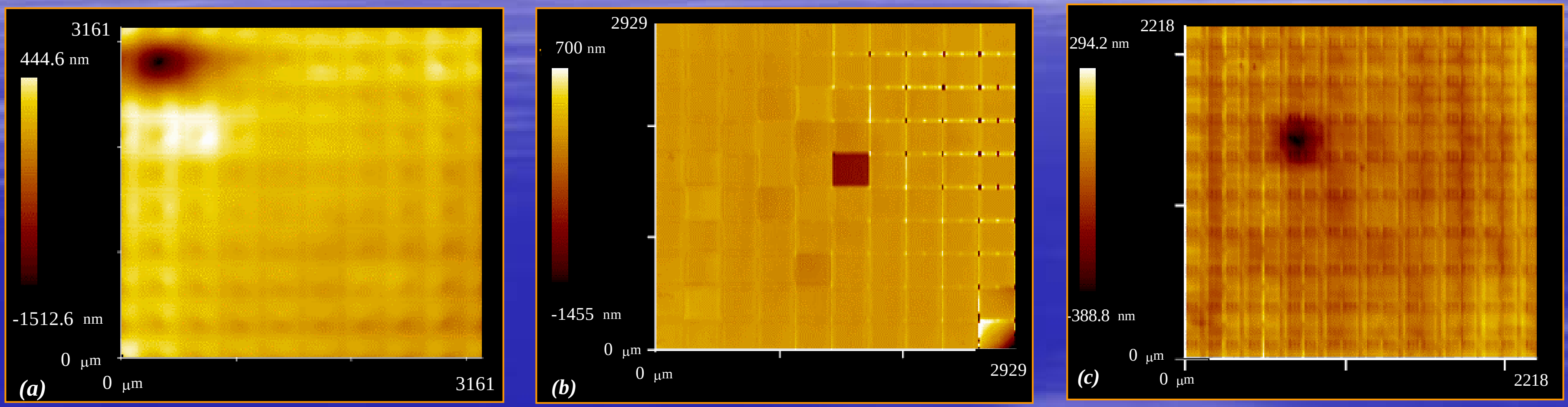

Interferometric surface maps of 10x10 actuator arrays with 1 actuator deflected

- 2 μm stroke
- Surface quality 50 nm rms
- 10 nm repeatability
- 7 kHz bandwidth
- $\lambda/10$ to $\lambda/20$ flatness
- < 1mW / Channel

Liquid crystal devices (LCD's = spatial light modulators)

- Pattern of phase delay is "written" onto back of LCD with light. Produces voltage change at each pixel, which changes index of refraction in liquid crystal.
- Incident light from AO system shines onto front of LCD. It reflects from the dielectric mirror, and double-passes through the liquid crystal.
- Spatial resolution is very high (480x480 pixels), hence it can correct a large number of spatial modes.
- But it behaves as purely a piston mirror, so correction per actuator is not as high as for a continuous mirror.

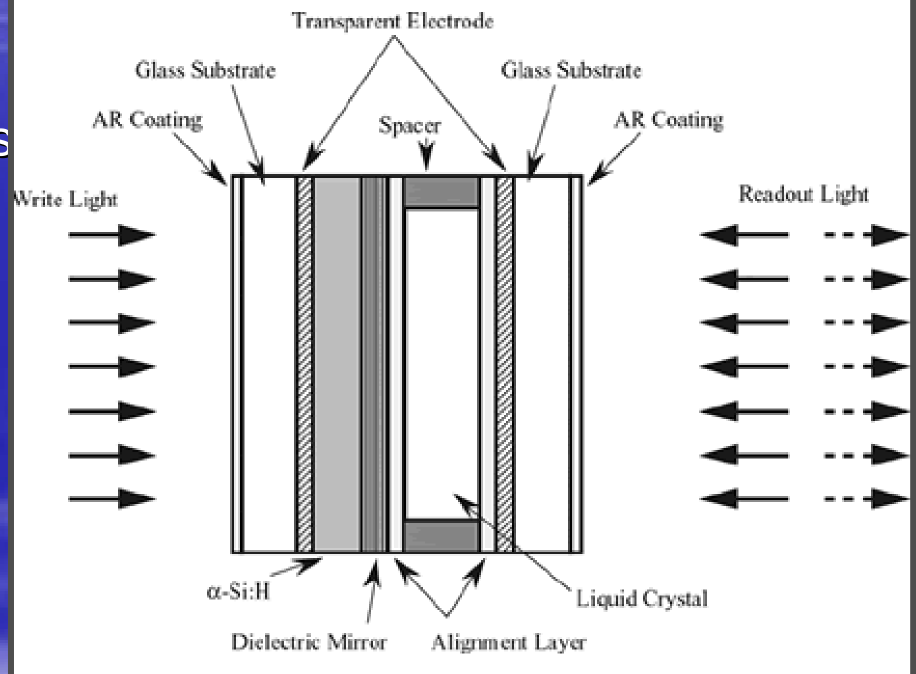

Cross section of the Hamamatsu LC-SLM

Problem: slow response time

Fitting error

$$\sigma_{fitting}^2 = a_F \, (d / r_0)^{5/3} \text{ rad}^2$$

- Physical interpretation: If we assume the DM does a perfect correction of all modes with spatial frequencies < 1 / r_0 and does NO correction of any other modes, then $a_F = 0.26$
- Equivalent to assuming that a DM is a "high-pass filter":
  - Removes all disturbances with low spatial frequencies, does nothing to correct modes with spatial frequencies higher than $1/r_0$

Fitting error and number of actuators

$$\sigma_{fitting}^2 = a_F \, (d / r_0)^{5/3} \ \text{rad}^2$$

DM Design	a_F	Actuators / segment
Piston only, square segments	1.26	1
Piston+tilt, Square segments	0.18	3
Continuous DM	0.28	1

Consequences: different types of DMs need different actuator counts, for same conditions

- To equalize fitting error for different types of DM, number of actuators must be in ratio

$$\left(\frac{N_1}{N_2}\right) = \left(\frac{d_2}{d_1}\right)^2 = \left(\frac{a_{F_1}}{a_{F_2}}\right)^{6/5}$$

- So a piston-only segmented DM needs

  (1.26 / 0.28)$^{6/5}$ = 6.2 times more actuators than a continuous face-sheet DM

- Segmented mirror with piston and tilt requires 1.8 times more actuators than continuous face-sheet mirror to achieve same fitting error:

$$N_1 = 3N_2 \,(0.18 / 0.28)^{6/5} = 1.8\, N_2$$

Summary of main points

- Deformable mirror acts as a "high-pass filter"
  - Can't correct shortest-wavelength perturbations
- Different types of mirror do better/worse jobs
  - Segmented DMs need more actuators than continuous face-sheet DMs
- Design of DMs balances stiffness and thickness of face sheet, stroke and strength of actuators, hysteresis, ability to polish mirror with high precision
- Large DMs are well proven (continuous face sheet, bimorph are used most often)
- MEMs DMs hold promise of lower cost, more actuators

High Contrast Imaging

The Center for Adaptive Optics is proposing the world's most powerful AO system

Extreme Adaptive Optics Planet Imager (ExAOPI):

- **A ~3000 actuator AO system for a 8-10m telescope**
- **Science goals:**
  - direct detection of extrasolar planets through their near-IR emission
  - characterization of circumstellar dust at 10x solar-system densities
- **Status: 2002-3 Conceptual design study**
  - System could be deployed in 2007
- **System to be funded by CfAO and external agency**
- **Constructed by LLNL, UCSC, CIT/JPL, UCB**

ExAOPI design concept

Parameter	Current Keck	ExAO
Subaperture size d	60 cm	~20 cm
Number of subapertures	241	~3000
DM size	~20 cm	~3 cm
System rate	670 Hz	2000 Hz
Controller	VMM	Predictive Fourier (or other advanced type)
Strehl ratio at 1.65 μm	0.2 / 0.4	0.9 - 0.95
Limiting magnitude	R ~ 13	R ~ 7 (R~10 aux. mode)

ExAOPI design concept

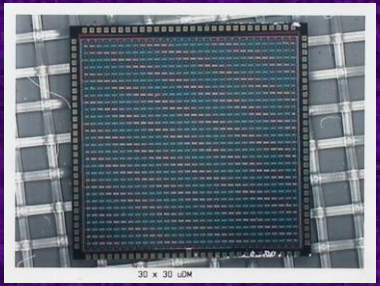

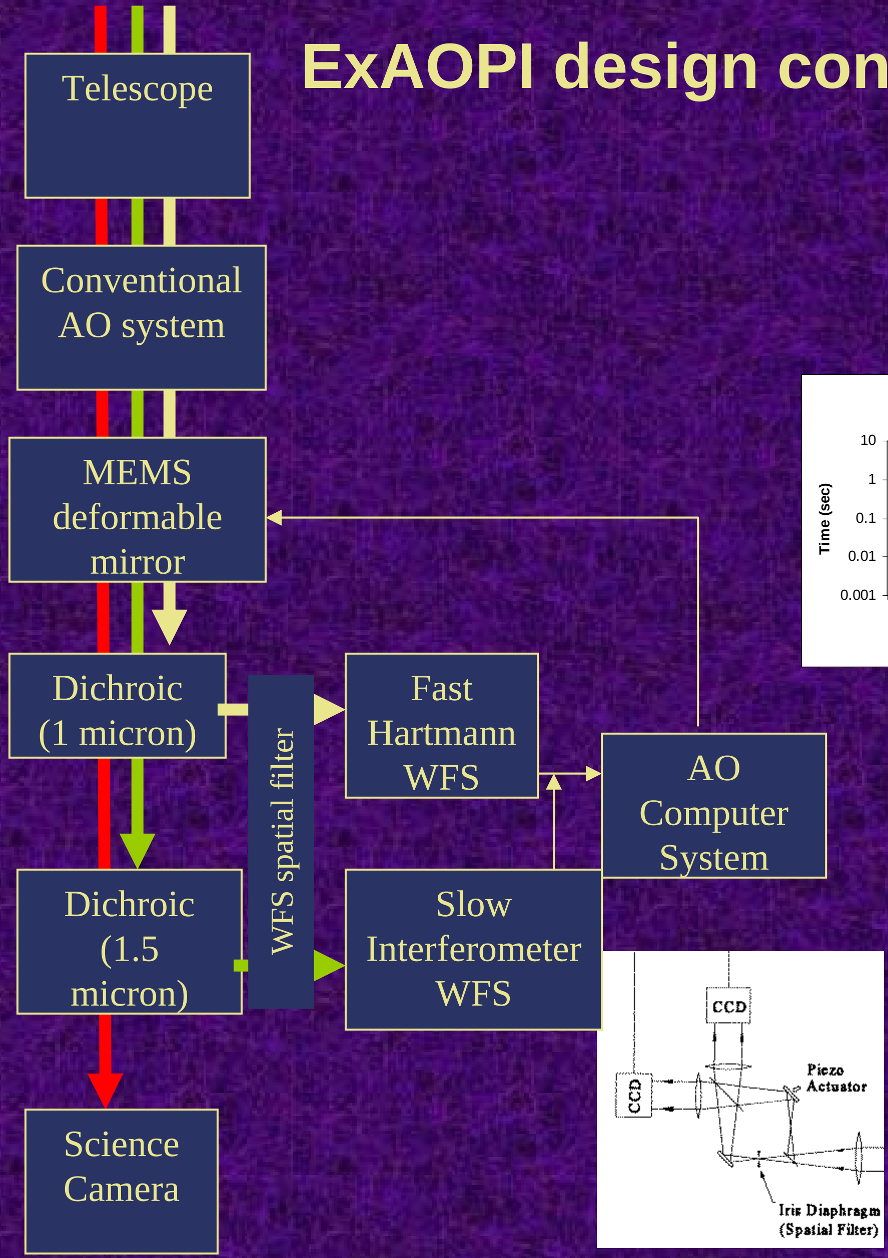

efficient control algorithms

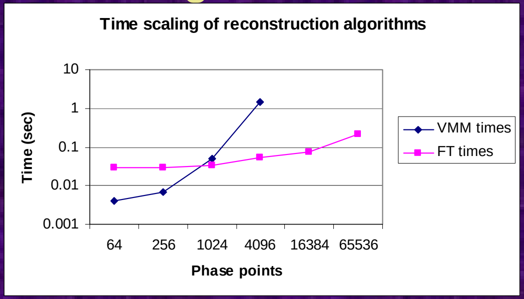

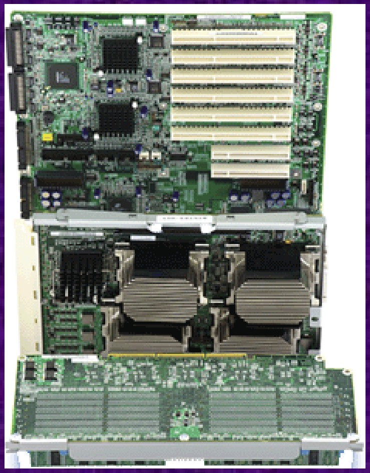

multiprocessor computer hardware

PSF shapes

- In principle, a perfect (or even near-perfect) deformable mirror should be able to reproduce all the low spatial frequencies in the wavefront error and dig out a deep null
- In practice, pupil-sensor systems never do this even in simulations

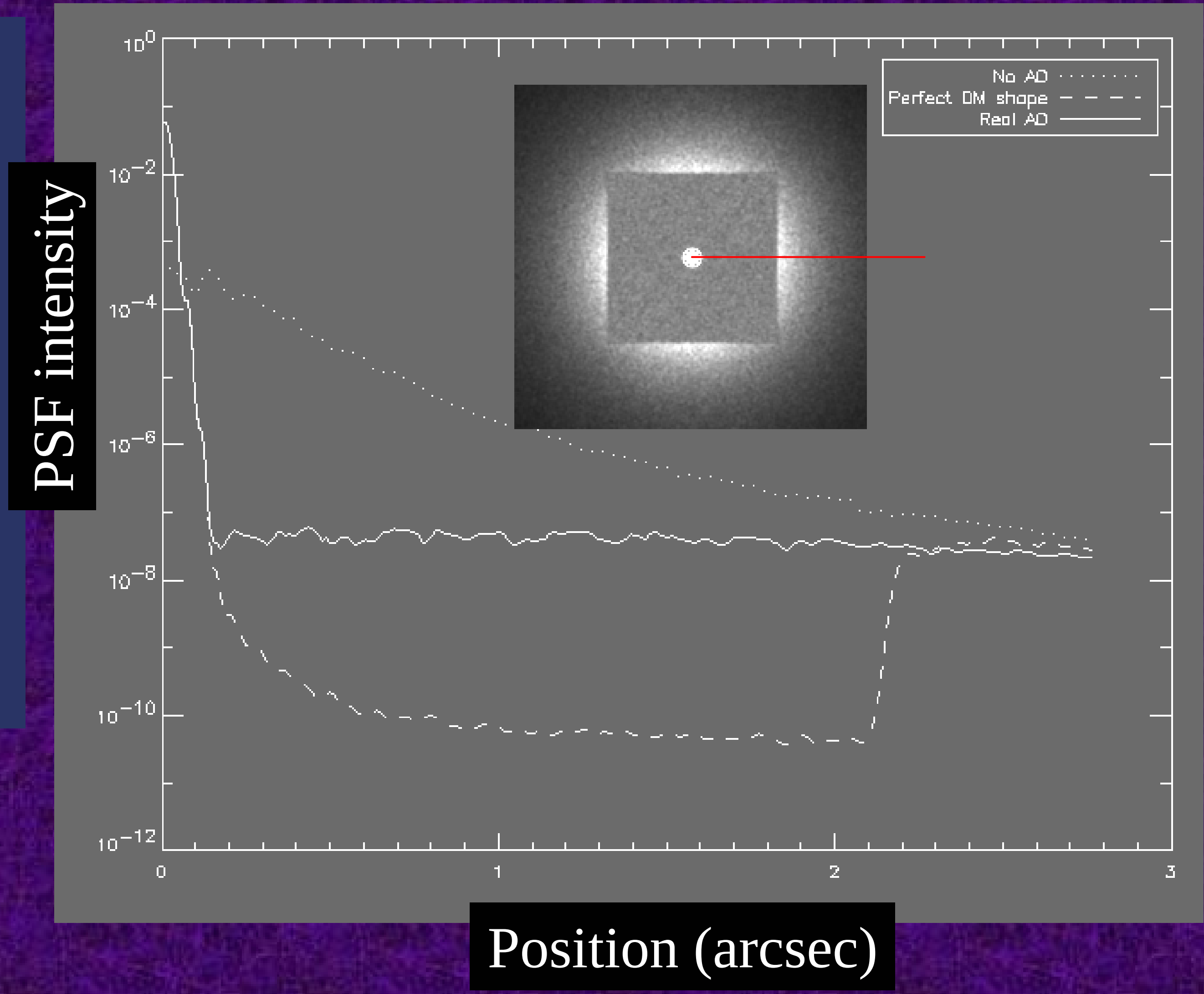

Spatial filter implementation

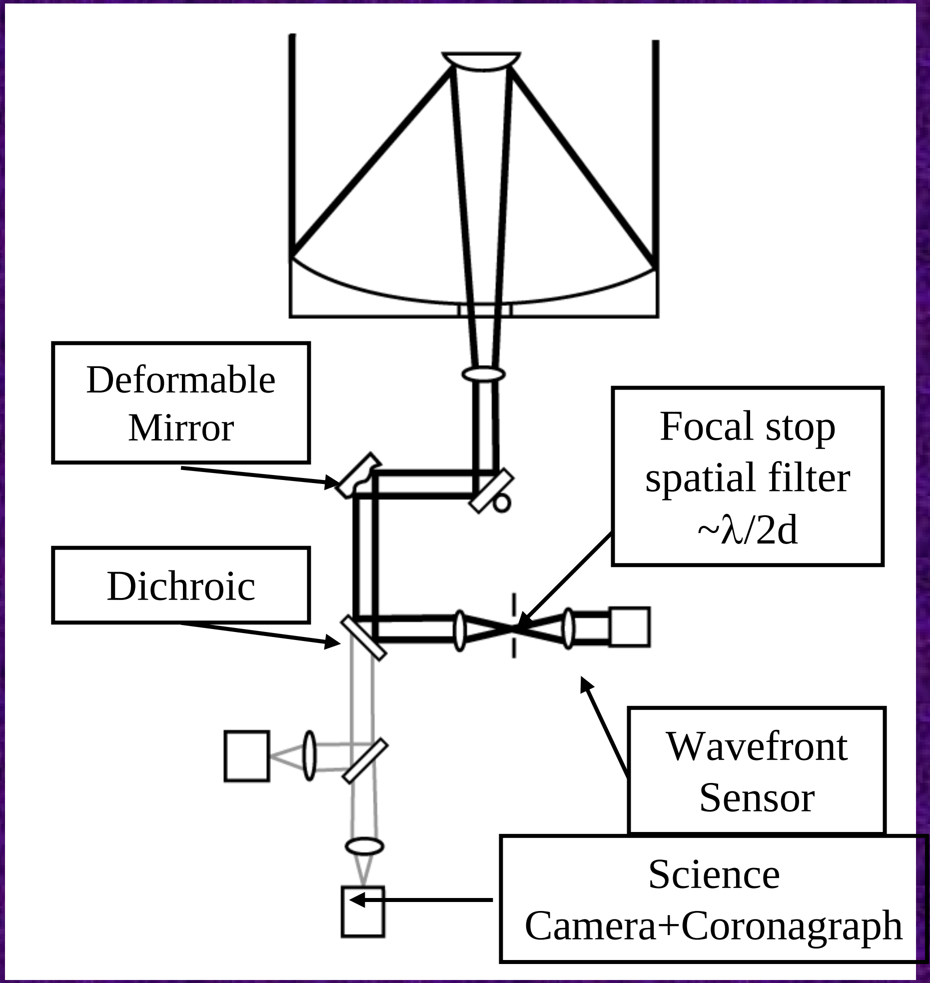

Discovery region darkness as a function of wavefront measurement and calibration error

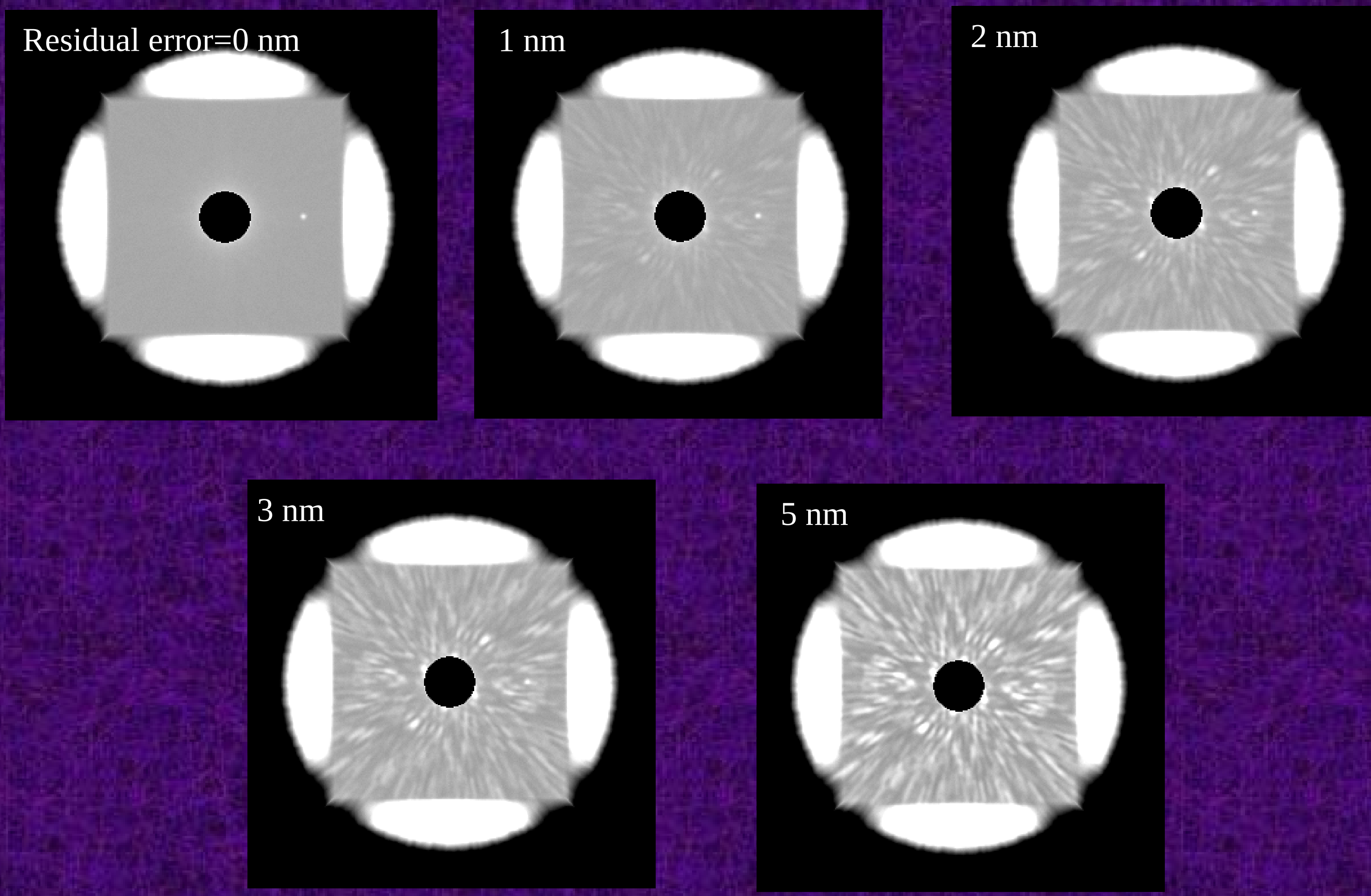

Summary

- Ground based adaptive optics systems correct for atmospheric turbulence
- Systems are in operation at several telescopes around the world – working mostly in the near IR
- Technology is challenging because of high speed & high precision requirements
- Planet imaging requires “extreme” adaptive optics – using a whole new generation of AO technologies